



FACULTY OF SCIENCE AND TECHNOLOGY

MASTER'S THESIS

Study programme/specialisation: Biological Chemistry	Spring / Autumn semester, 2018.....
Author: Samuel James Danby	Open/ Confidential
The Effects of Metformin on the Metabolism of Colorectal Cancer Cell Lines SW948 and SW1116	
Programme coordinator: Hanne Røglund Hagland Supervisors:	
Credits: 60	
Number of pages:60 +16 supplemental Keywords: Colorectal Cancer, Metformin, OCT1, Metabolism, Stavanger 12/06/18	

The Effects of Metformin on the Metabolism of Colorectal Cancer
Cell Lines SW948 and SW1116

Samuel James Danby

Acknowledgements

My supervisor Hanne Røland Hagland deserves great recognition for being a vital part of my masters study. Firstly for giving me the opportunity to take this research project at the Centre for Organelle Research (CORE), and giving me the freedom to blossom but always providing support when needed. Hanne has ensured that my research has been achievable but challenging, ensuring my development in cancer research and as a person in a laboratory environment.

Hanne has surrounded herself with very good team who have offered their experience to help with my research. I took the project over from Abdelnour Alhourani and Ansooya Bokil, and both made the continuation smooth by offering their support and time to ensure that I could perform the cell culture techniques required and also collaborated on additional projects to expand my abilities in the lab. Julie Nikolaisen and Tia Tidwell have also both been available to go through techniques with me and answered any questions that I had both on my project and general lab questions and I greatly appreciate their efforts during my research.

I was lucky to begin my year along with other masters students, and having Cecilie Lindseth, Aleksandra Szwedo and Hina Ahmad around not only for continued support and working together on projects and techniques but also the invaluable friendships I have gained also.

Finally, and I will be told most important, my family. Starting the year with a new born baby would always have obstacles but I have been lucky enough to spend the last month at home with my little one year old Frida. I am grateful to my girlfriend Evelyn who has given me continued support during my studies and ensured I always have time to perform research, the former definitely did not.

Thank you to CORE, and UiS for this great opportunity and project I have had the chance to be a part of.

Abstract

Metformin is an anti-diabetes drug with cancer preventative capabilities, which is widely studied to help develop treatment to aid future colorectal cancer prevention and recovery. This studies aims were to assess the phenotypes of colorectal cancer cell lines SW948 and SW1116, including detailed analysis of the metabolic shift achieved by the cells to continue growth when stress is applied, via varied metformin concentrations and glucose concentration adjustments. An alternative focus was to locate and achieve quantitative data on how metformin influences expression of organic cation transporter1, which is responsible for transporting metformin into the cell. The results proposed that the effects of metformin on colorectal cancer cells are influenced by cell line and glucose concentrations. When using metformin as a therapeutic agent, taking into consideration the metabolic phenotype of the cancer cell and glucose concentrations to ensure a more unique course of treatment.

1 Contents

Abstract	4
Abbreviations	7
List of Tables	8
List of Figures (make shorter in contents)	9
1. Introduction and literature review	13
1.1 Cell Metabolism	13
1.1.1 Cancer Metabolism	14
1.1.2 Colorectal Cancer	14
1.2 Metformin And Cancer	14
1.2.1 Metformin	14
1.2.2 Metformin And Cancer	15
1.2.3 Metformin and Glucose	16
1.3 Biomarkers	16
1.3.1 Biomarkers In Cancer Research.....	17
1.3.2 Organic Cation Transporter.....	17
2. Research aims	19
Primary aims	19
Secondary aim	19
3 Methods and materials	20
3.1 Solutions And Kits	20
3.1.1 Cell Lines.....	20
3.1.2 Solutions and Kits	21
3.2 Culturing Cells	22
3.2.1 Cell Incubation.....	22
3.2.2 Culturing Conditions	22
3.2.3 Revival Of Cells.....	22
3.2.4 Bringing Adherent Cells To Suspension	23

3.2.5	Cell Counting.....	23
3.2.6	Passage Of Cells	24
3.3	Cell Growth And Doubling Time.....	25
3.4	Seahorse Phenotype Analysis.....	26
<i>Figure 6 Seahorse XFp flux cartridge layout. Ports A-D for drugs to be introduced into the analysis. Image taken from the Millipore Seahorse protocol</i>		
<i>26</i>	<i>.....</i>	<i>27</i>
3.5	BrdU Proliferation Assay	29
3.6	Alamar Blue Assay	30
3.7	Immunocytochemistry: Confocal Imaging of OCT1	31
3.7.1	Seeding.....	31
3.7.2	Staining.....	31
3.7.3	Imaging	32
4	Results.....	34
4.1	Growth Of SW948 And SW1116.....	34
4.1.1	SW948 Proliferates Quicker Than SW1116	34
4.2	Glucose Concentrations have an effect on the Metabolic Phenotype of Colorectal Cancer Cells Lines SW948 and SW1116	36
4.3	Increase in Concentrations of Metformin Inhibit Colorectal Cancer Cell Growth	38
4.3.1	BrdU Proliferation Assay	38
4.3.2	Alamar Blue Viability Assay	40
4.4	OCT1 Responsible for Transporting Metformin Is Located on the Outside of the Cell	42
4.4.1	Confocal Imaging of OCT1	43
4.4.2	Oct-1 Expression Changes With An Increase In Concentration Of Metformin	52
5	Discussion	54
6	References	60

Abbreviations

ATP : Adenosine Triphosphate

TCA: Tricarboxylic Acid

NADH: Nicotinamide adenine dinucleotide

OXPPOS: Oxidative phosphorylation

FH: Fumarate Hydratase

SDH: Succinate Dehydrogenase

CRC: Colorectal Cancer

cAMP: Cyclic Adenosine Monophosphate

OCT1: Organic Cation Transporter1

DMEM: Dulbecco's Modified Eagle Medium

FBS: Foetal Bovine Serum

MTS: Mito Stress Test

GTS: Glycolysis Stress Test

BCA: Bicinchoninic Acid

PFA: Paraformaldehyde

ROI: Regions of Interest

List of Tables

Table 1 and kits used and Reagents the technique performed. ICC is immunocytochemistry 21

Table 2 List of compounds to be added to the mito stress and glycolysis stress test with dilutions amounts and how much to be added to each port on the Seahorse plate. *2-DG is added directly from the 1M stock28

Table 3 Conditions used for Alamar Blue, each low glucose and high glucose concentration was tested with five concentrations of metformin (0.5mM, 1.0mM, 3.0mM, 5.0mM 10.0mM) and a control with no metformin.....30

Table 4 Images taken on the Leica Confocal Microscope after analysis using Leica Application Suite 2.0 to add regions of interest to collect data of OCT1 in yellow using antibody SLC22A compared to the nucleus in blue stained with hoeschst in colorectal cancer cell line SW948. The treatment conditions shown are 6 hours, 12 hours, 24 hours and 48 hours using high glucose labelled HG and low glucose labelled LG with metformin treatments of 0.5mM and 3.0mM including a control which was used to compare the changes in OCT1 using the regions of interest.44

Table 5 Images taken on the Leica Confocal Microscope after analysis using Leica Application Suite 2.0 to add regions of interest to collect data of OCT1 in yellow using antibody SLC22A compared to the nucleus in blue stained with hoeschst in colorectal cancer cell line SW948. The treatment conditions shown are 6 hours, 12 hours, 24 hours and 48 hours using high glucose labelled HG and low glucose labelled LG with metformin treatments of 0.5mM and 3.0mM including a control which was used to compare the changes in OCT1 using the regions of interest. The images were taken to determine the location of OCT1.48

List of Figures

Figure 1 Cell metabolism in cancer cells. Tricarboxylic acid cycle (TCA) actions in the mitochondria. The glucose enters via a transporter enters the cell as pyruvate via glucose-6-phosphase. The PDK and PDH in the mitochondria can be targeted for cancer therapy. IDH2, FH and SDH are all present due to the shift in mechanisms due to it being a cancer cell ¹	13
Figure 2 - Image of a mitochondria in the cell with the areas involved in the ECT highlighted, showing locations of Complex I, where metformin enters the mitochondria. Image: cell signalling.....	15
Figure 3- Showing metformin's entrance into the cells via OCT1 following inhibition of complex I which affects the cells efficiency to produce ATP ¹³	18
Figure 4 Hemocytometer with 1mm 16 square areas highlighted in red (Image: stemcell technologies).....	24
Figure 5 Seahorse XFp cell culture miniplate. Wells B, C and D were used for high glucose conditions with appropriate metformin treatment and E, F and G were used for the low glucose conditions with metformin treatments. Wells A and H were used for control without cells. Image taken from the Millipore Seahorse protocol ²⁶	26
Figure 6 Seahorse XFp flux cartridge layout. Ports A-D for drugs to be introduced into the analysis. Image taken from the Millipore Seahorse protocol ²⁶	27
Figure 7 Layout of the five region of interest's used to quantify data in LASX of the ratio of OCT1:Hoeschst from the images taken on the Leica TCS Confocal Microscope using the 20x objective	32
Figure 8 Images of cells lines SW948 and SW1116 showing growth differences. (A) SW948 2 hours after passaging, (B) SW948 24 hours, (C) SW948 48 hours, (D) SW1116 2 hours after passaging, (E) SW1116 48 hours after passaging	34

Figure 9 - Cell growth of SW1116 & SW948 over 72 hours based on initial seeding of 100,000 cells of SW948 and 200,000 of SW1116.....35

Figure 10 Wave 2.6.0 results from the seahorse XFp analyser. Mito stress test on colorectal cancer cell line SW948 in high glucose and low glucose concentrations under three different treatments of metformin. (A) Control with no metformin, (B) 0.5mM of metformin, (C) 3.0mM of metformin. The graphs represent OCR vs. ECAR normalised using micrograms of protein present in the samples.....36

Figure 11 Wave 2.6.0 results from the seahorse XFp analyser. Glycolysis stress test on colorectal cancer cell line SW948 in high glucose and low glucose concentrations under three different treatments of metformin. (A) Control with no metformin, (B) 0.5mM of metformin, (C) 3.0mM of metformin. The graphs represent OCR vs. ECAR normalised using micrograms of protein present in the samples.....37

Figure 13 Wave 2.6.0 results from the seahorse XFp analyser. Mito stress test on colorectal cancer cell line SW1116 in high glucose and low glucose concentrations under three different treatments of metformin. (A) Control with no metformin, (B) 0.5mM of metformin, (C) 3.0mM of metformin. The graphs represent OCR vs. ECAR normalised using micrograms of protein present in the samples.....37

Figure 12 Wave 2.6.0 results from the seahorse XFp analyser. Glycolysis stress test on colorectal cancer cell line SW1116 in high glucose and low glucose concentrations under three different treatments of metformin. (A) Control with no metformin, (B) 0.5mM of metformin, (C) 3.0mM of metformin. The graphs represent OCR vs. ECAR normalised using micrograms of protein present in the samples37

Figure 14 Results from BrdU proliferation assay on colorectal cancer cell line SW1116. Each result for the respective metformin treatment is compared against the control for each high glucose and low glucose concentrations using the absorbance read on the spectramax plate reader.....38

Figure 15 Results from BrdU proliferation assay on colorectal cancer cell line SW948. Each result for the respective metformin treatment is compared against the control for each

high glucose and low glucose concentrations using the absorbance read on the spectramax plate reader.....	39
Figure 16 Results from alamar blue viability assay on colorectal cancer cell line SW1116. Each result for the respective metformin treatment is compared against the control for each high glucose and low glucose concentrations using the fluorescence read on the Spectramax plate reader	40
Figure 17 Results from alamar blue viability assay on colorectal cancer cell line SW948. Each result for the respective metformin treatment is compared against the control for each high glucose and low glucose concentrations using the fluorescence read on the Spectramax plate reader	41
Figure 18 Images of the location of OCT1 in yellow to the nucleus in blue, images were analysed on the Leica LASX to show location of OCT1. (A-C) SW1116 High Glucose control sample after 48 hours, showing staining of the nucleus in blue, staining of OCT1 in yellow and overlap of both stains together (D-F) SW1116 High Glucose with 0.5mM metformin treatment after 48 hours showing staining of the nucleus with hoeschst in blue, staining of OCT1 in yellow and overlap of both stains together. Images were taken on the Leica Confocal imaging microscope with the 63x objective. The nucleus was stained using Hoechst and OCT1 with primary antibody <i>SLC22A1</i> . The cells were not permeabilised.	42
Figure 19 Image of sample taken for SW1116 Low Glucose 3.0mM after 48 hours. (A) Stained nucleus as blue (B) Stained OCT1 as yellow (C) Overlay of the images. Images were taken using 20x objective on the Leica Confocal Microscope.	43
Figure 20 Ratio of OCT1 against cell nucleus using data from quantification on the Leica Application Suite using five regions of interest. The results are presented as a percentage compared to the control sample for concentrations of metformin (0.5mM, 3.0mM and a control) for high glucose (HG) and low glucose (LG) concentrations.	52
Figure 21 Ratio of OCT1 against cell nucleus using data from quantification on the Leica Application Suite using five regions of interest. The results are presented as a percentage	

compared to the control sample for concentrations of metformin (0.5mM, 3.0mM and a control) for high glucose (HG) and low glucose (LG) concentrations.53

1. Introduction and literature review

1.1 Cell Metabolism

The mitochondria play a vital role in the production of Adenosine Triphosphate (ATP) as a by-product of the tricarboxylic acid cycle (TCA), to help power the cell. The TCA cycle also produce Nicotinamide Adenine Dinucleotide (NADH) and Flavin Adenine Dinucleotide (FADH²) which deliver their electrons to the Electron Transport Chain (ETC) for assistant with oxidative phosphorylation (OxPhos) which, produces ATP^{1,2}.

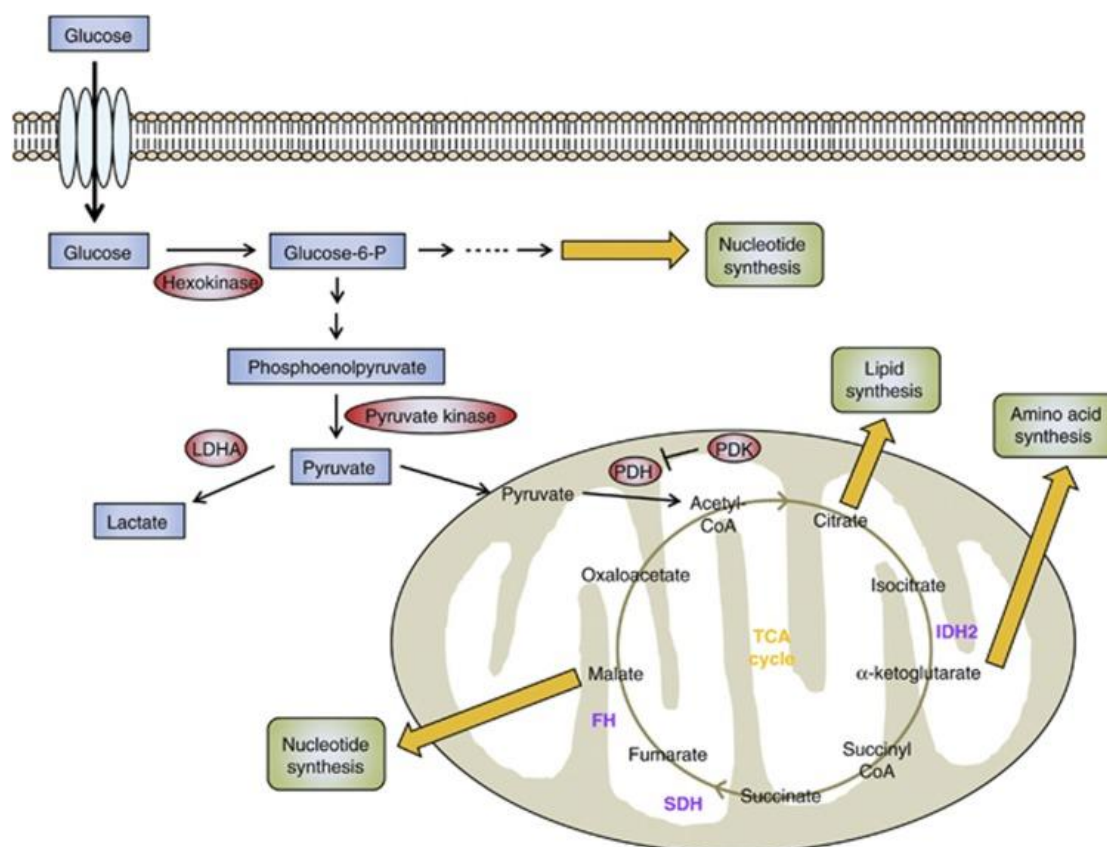


Figure 1 Cell metabolism in cancer cells. Tricarboxylic acid cycle (TCA) actions in the mitochondria. The glucose enters via a transporter enters the cell as pyruvate via glucose-6-phosphase. The PDK and PDH in the mitochondria can be targeted for cancer therapy. IDH2, FH and SDH are all present due to the shift in mechanisms due to it being a cancer cell¹.

1.1.1 Cancer Metabolism

Cancer is the word used to describe abnormal cell growth, and they behave differently to normal cells. Normal cells use glycolysis to produce pyruvate from glucose for energy that enters the TCA cycle, whereas cancer cells use more glucose and produce lactic acid. This is a shift in the metabolism and is known as the Warburg effect². As highlighted in purple in the mitochondria in figure 1, the mutations in Succinate Dehydrogenase (SDH) and Fumarate Hydratase (FH) can cause build up in succinate and fumarate in the TCA cycle which may be linked to changes in mitochondrial respiration in cancer cells⁵.

Cancer cells favour glycolysis and have adapted to function without the presence of oxygen and its energy production system OxPhos; which helps cancer cells grow without a fully functioning mitochondria, but also often prefer glycolysis even in the presence of oxygen⁶.

1.1.2 Colorectal Cancer

The third leading cancer for mortality, is colorectal cancer (CRC)⁴. Older age, family history of CRC, particular heredity conditions and lifestyle choices such as alcohol consumption and diet are risk factors for CRC^{7,8}.

1.2 Metformin And Cancer

1.2.1 Metformin

Metformin is most famously known as a leading drug used for treatment of type II diabetes, offering an effect to help prevention of diabetes; this is achieved due to the weight loss properties it holds, opposed to the weight gain affects often seen in diabetes treatments⁹.

Ultimately, metformin a popular choice of drug due to the ability to reduce gluconeogenesis in the liver without reducing its ability to produce insulin but the mechanisms behind the inhibition of gluconeogenesis is unknown, with multiple hypothesis offered¹⁰.

1.2.2 Metformin And Cancer

Metformin has been found to suppress the growth of cancer stem cells, particularly in the respiratory chain complex I; an area in the mitochondria where cells produce ATP¹¹. Figure 2

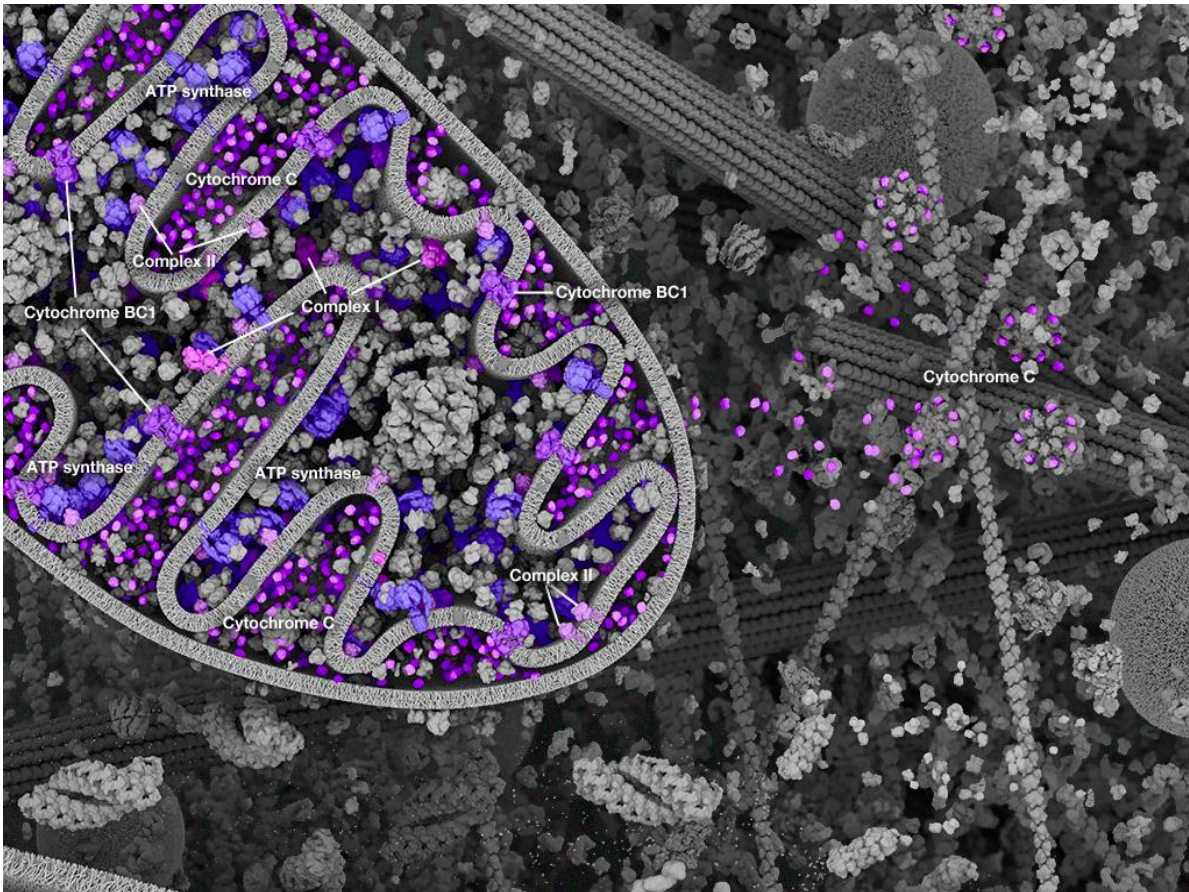


Figure 2 - Image of a mitochondria in the cell with the areas involved in the ETC highlighted, showing locations of Complex I, where metformin enters the mitochondria. Image: cell signalling

demonstrates the pathway taken by metformin to alter the function of the ETC indicates that after entering the mitochondria it causes decreased NADH oxidation via complex I. This reduced ETC function and obstructs the TCA cycle effectively hindering the cells ATP production. The result of this process activates AMPK by reducing mitochondrial energy output^{10,12}, decreasing signalling of cAMP/PKA and decreasing gluconeogenesis and most importantly increase glycolysis^{13,14}.

Figure 1 above presents an overview of the mitochondria highlighting the areas which are active for the ETC to function, showing where metformin disrupts the mitochondria at complex I.

Research performed regarding the effects of metformin on different colorectal cancer cell lines, found that metformin affects each independently and some cell lines can be more resistant than others to metformin and its ability to inhibit growth in the cells¹¹. Thus far, trials involving metformin for cancer treatment has not been successful, but data has been collected for tumours in different areas of the body, with more progress in some than others and each requiring different concentrations of metformin¹⁵.

1.2.3 Metformin and Glucose

Metformin is tightly linked with glucose production levels in the blood and helps promote successful homeostasis of insulin. Tests on metformin concentrations are being performed on colorectal cancer cells, results can differ between each cell line due to stages of cancer and type. Also the drug's effect can differ between concentrations of glucose used for analysis. Depending on the origin of the cancer cell, glucose may be suitable in higher concentrations. Cell lines from the same cancer type exhibit different growth behaviours depending on glucose concentrations^{10,16}. Furthermore, cells proliferate differently depending on oxygen levels available, with research showing that changes in the oxygen levels has a direct effect on cell growth. Glucose has an influence on growth also, some cancer cell lines will be more glycolytic and use glucose for energy and some have an OxPhos metabolic profile¹⁷.

1.3 Biomarkers

A biomarker was early described as a structure or substance that can help determine the processes as to why disease may occur, and its mechanisms. Biomarkers are used more and more in current day research. Biomarkers are becoming a more automatically approved method when performing clinic research, although there are libraries of use of particular biomarkers it is vital that they are continued to be validated and reassessed to confirm their

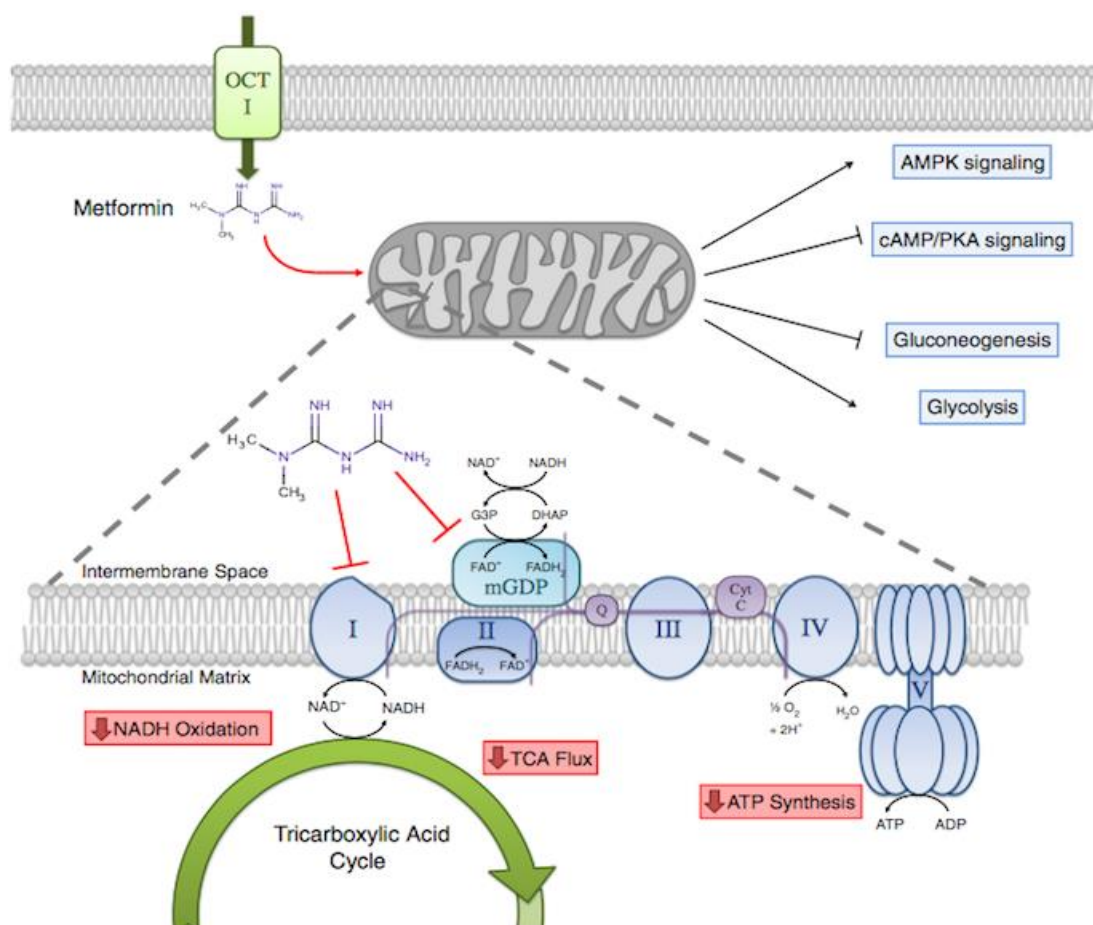
validity. They will continue to help learn more about the diseases that are most destructive and this includes development of drugs¹⁸.

1.3.1 Biomarkers In Cancer Research

Biomarkers are useful when performing trials to help give more information to improve the understanding of diseases such as cancer. Although few have been implemented into clinical practice, biomarkers can be used to help identify classifications of cancer and also grade/stages of cancer. This can be critical information to have access to when selecting treatment¹⁹.

1.3.2 Organic Cation Transporter

Organic cation transporter 1 (OCT1) plays a role in the uptake of metformin, and is a suitable candidate for analysis to help achieve a better understanding of metformin and its ability to



inhibit colorectal cancer cell proliferation²⁰. This transporter of metformin allows the drug to cross the cell membrane and assemble at the mitochondria as they affect the effectiveness of complex I in the ETC. Although research on OCT in the colon is not extensive, research has shown that OCT is important for the uptake of drugs including metformin and also thiamine in the liver^{21,22}.

Figure 3- Showing metformin's entrance into the cells via OCT1 following inhibition of complex I which affects the cells efficiency to produce ATP¹³.

OCT1 is very highly expressed in the liver and therefore so much research is available on the transporter in the hepatic organ, with lower levels expressed in other organs including the intestines. Although suggested to be 'liver-specific', it is helpful to colorectal cancer research to further investigate the mechanisms in the intestines²³.

2. Research aims

Primary aims

The research will assess the phenotype differences between colorectal cancer cells lines SW948 and SW1116, and what role metformin has on their metabolic response.

The glucose concentrations in which cancer cell lines SW948 and SW1116 favour for growth. Using both high glucose 4.5g/L (25mM) and physiological / low glucose 1g/L (5mM) to perform trials on the two cell lines, and conclude if either influences the cells response to metformin, and are there any characteristics to compare between the two cell lines.

Secondary aim

The expression in the Organic Cation Transport1 (OCT1) difference between the cells lines, and changes under the treatment and growth conditions mentioned in the major and minor aims.

3 Methods and materials

3.1 Solutions And Kits

3.1.1 Cell Lines

Two cell lines were used for this paper, both product numbers and information on the origin of the samples are taken from European Collection of Authenticated Cell Cultures (ECACC)

<i>Cell line</i>	<i>Product number</i>
<i>SW948</i>	91030714
<i>SW1116</i>	87071006

3.1.1.1 *SW948*

Derived from a grade III adenocarcinoma of the colon of an 81-year-old Caucasian female.

3.1.1.2 *SW1116*

Derived from a grade II adenocarcinoma of the colon extending into the muscularis from a 73-year-old Caucasian male.

Both cells lines were cultured using Dulbecco's Modified Eagle Medium (DMEM) with the supplement additions of 10% Foetal Bovine Serum (FBS), 2mM/l (0.584 g/l) L-Glutamine plus antibiotics Penicillin (100 U/ml) and Streptomycin (10µg/ml)

3.1.2 Solutions and Kits

Table 1 and kits used and Reagents the technique performed. ICC is immunocytochemistry

<u>Solution and Kits used</u>	<u>Manufacturer</u>	<u>Catalogue number</u>	<u>Technique</u>
96 Well Plates Black Coated with Clear Bottom	Corning	3603	96-well Plate reader
Tryphan Blue	Amresco	K940 100ML	Cell counting
Muse C&V Assay Kit	Muse	MCH600103	Cell counting
Burker Counting Chamber	Marienfeld-superior		Cell counting
DMEM No Glucose Media	Corning	17-207-CVR	Cell culture
Glucose Powder	Borrowed from another lab		Cell culture
Trypsin/EDTA	Sigma	T4049- 500ML	Cell culture
T75cm² Culture Flasks with Vented Cap	Corning	353136	Cell culture
Penicillin-Streptomycin	Biowest	L0018-18	Cell culture
15ml Centrifuge Tubes	VWR		Cell culture
50ml Centrifuge Tubes	VWR		Cell culture
Sanyo CO₂ Incubator	Sanyo	MCO- 18AIC	Cell culture
T25cm² Culture Flasks	Corning	353108	Cell culture
Phosphate Buffered Saline	Sigma	P4417- 50TAB	Cell culture
DMEM 4.5g/L Glucose Media	Corning	15-017-CVR	Cell culture
L-Glutamine 200mM	Corning	25-005-CL	Cell culture
6-Well Plates with Clear Flat Bottom	VWR	734-2323	Cell doubling time
BrdU Cell Proliferation Assay Kit	Millipore	2570	Cell proliferation
Alamar Blue	Biosciences	786-922	Cell viability
Leica TCS SP8 Confocal Microscope	Leica		ICC: Confocal Imaging
Leica LASX Application Software	Leica		ICC: Confocal imaging
μ-Slide 8 Well	Ibidi	80826	ICC: Seeding
Goat Anti Mouse Secondary Antibody Fluor 568	Introgen	A11004	ICC: Staining
Tween-20	Melford	P1362	ICC: Staining
Foetal Calf Serum	Borrowed from another lab		ICC: Staining
Primary mouse antibody OCT1 SLCC2A	Genetex	GTX80400	ICC: Staining
Hoechst 33342	Borrowed from another lab		ICC:Staining
Seahorse XFp Analyser and consumables	Agilent		Seahorse assay

3.2 Culturing Cells

3.2.1 Cell Incubation

The growth conditions for the cells are in an incubator at 37°C, in an atmosphere of 5% carbon dioxide (CO₂). This ratio of oxygen (O₂) and CO₂ are to remain consistent; too high can be fatal and too low can cause a halt in growth²⁴.

3.2.2 Culturing Conditions

The cells are grown in two different glucose environments to assess the differences in growth.

3.2.2.1 High Glucose Media

The cells are constantly grown in DMEM media with additional supplements and high glucose of 4.5g/L, which is consistent to offer suitable comparisons to other studies undertaken.

3.2.2.2 Physiological/ Low Glucose Media

DMEM media with additional supplements and 1g/L of glucose is used to replicate the environment the cells would typically be present in clinical environments.

3.2.3 Revival Of Cells

SW1116 cells at passage number 8 (P8) and SW948 at P9 were taken from the Centre of Organelle Research (CORE) cryo-tank where they have been frozen at -185°C in liquid nitrogen in a 1ml vial. The vials were held in a 37°C water bath until they thawed, then they were instantly added to a 75 cm² (T75) flask containing 37°C medium and straight into the incubator. The next day, they were brought to suspension and centrifuged at 900rpm for 5

minutes, the supernatant removed of freezing media and re-suspended into new 37°C cell media and added to a new T75 flask.

3.2.4 Bringing Adherent Cells To Suspension

For most of the experiments that were performed, the cells needed to be suspended in cell media. This is because the cells are adhered, and they attach to the flask in which they are being cultured. The media was aspirated out the flask, and 37°C PBS was added to wash, rocking the flask to distribute evenly and aspirate out. 3ml of 37°C trypsin is added and then the flask is put in the incubator until the cells attach (5-7minutes for SW948 and 10-15 minutes for SW1116). 4ml of 37°C growth media was added and mixed with a pipette to break up any cell clumps. The suspension was added to a 15ml falcon tube and centrifuged for 5 minutes at 900rpm. The supernatant is removed and washed with PBS, spun again and fresh media is added. Then the cells were ready for experiments.

3.2.5 Cell Counting

3.2.5.1 Hemocytometer

When the cells reached 70% confluency they were brought to suspension (3.2.4). 100ul of the suspension added to sterile Eppendorf tube, then 100ul of trypan blue was added into the tube and pipetted up and down to mix together creating a 50/50 ratio. The Bürker Chamber hemocytomer glassware and cover slip was washed with distilled water (DH₂O). 20ul of the solution was added to each chamber of the counter and placed under the microscope at 10X. In each corner are 16 squares of 4x4 (1mm). Single cells were counted from one corner of the 1mm area until all 16 squares had been counted, this giving a total cell count for that corner, and all 4 corners of the counter (shown in red on figure 3) the average was used to find total cells per 1ml of suspension.

Cells per 1ml = (Average of four counts x 2 (dilution factor of trypan blue)) x 10000

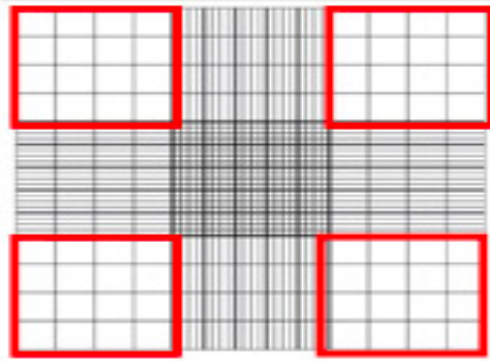


Figure 4 Hemocytometer with 1mm 16 square areas highlighted in red (Image: stemcell technologies)

3.2.5.2 Muse Cell Analyser

The Millipore Muse Cell Analyser was an alternative and more precise method of counting cells, plus it offered a much quicker result time allowing for many cell suspensions to be counted in a shorter period of time. The count was done using the viability test kit from Millipore where the live cells were separated from the apoptotic to give a cell count. It was important to ensure the cells were suspended evenly as the muse analyser counts single cells. The nuclear dye stained the live cells and the dead cells were stained by the viability dye. This gave distinctions between both when counted, and the debris was removed with a negative stain. The Muse Analyser was used to count all the cells samples when performing any test²⁵.

3.2.6 Passage Of Cells

After being brought to suspension, the cells were distributed evenly in a 15ml falcon tube by pipetting up and down with a 1000 μ l (1ml) pipette, and added cells from the cell suspension to new DMEM growth media at 37 $^{\circ}$ c in a T75 flask.

The ratio of cell suspension into the new media varied depending on cell line; SW948 required a 1:4-1:7 (cell suspension: growth medium). SW1116 at a ratio of 1:3 due to their longer growth time.

3.3 Cell Growth And Doubling Time

This assays was done four times; SW1116 at P11, P13, P14 and P17. SW948 at P12, P15, P16 and P20 respectively. For each biological replicate 1,000,000 (10^6) cells were suspended in 10ml of both high and physiological media, the suspension was added to three separate Corning Multi-well Clear Bottom 6 well plates at 1ml per well so that 9 wells in total contained 100,000(10^5) cells for each high and physiological glucose. Each well then was topped up with 2ml of respective media so that each well had 3ml total of media and 100,000 cells. This gave three technical replicates for both glucose concentrations to be counted after 24, 48 and 72 hours. After the time periods of 24, 48 and 72 hours the media was removed, washed, and trypsin was added to the wells to detach and then counted using the Millipore Muse Cell Analyser to count the cells. The count was then compared to the initial seeding density of to calculate doubling time. Doubling time is calculated as

$$\text{Doubling time} = \frac{\text{Time period} \times \log(2)}{\log(n_f) - \log(n_i)}$$

n_f = final count

n_i = initial seeding number

3.4 Seahorse Phenotype Analysis

Metabolic assays were performed on the Seahorse XFp Analyser to determine the phenotype of cell lines SW948 and SW1116 to analyse differences between them and also compare how glucose concentrations can change how they get energy. Seahorse XFp Analyser and 8-well Seahorse XFp Cell Culture Miniplates were used for analysis, 1 miniplate was needed for each condition being analysed. Each SW948 and SW1116 were used at p17 in high and low glucose concentrations and at 3 metformin concentrations (0.0mM control, 0.5mM and 3.0mM). Cells were seeded into the miniplate, 10000 cells were seeded for SW948 and 20000 for SW1116 in 100µl of high glucose media for the cells to attach.

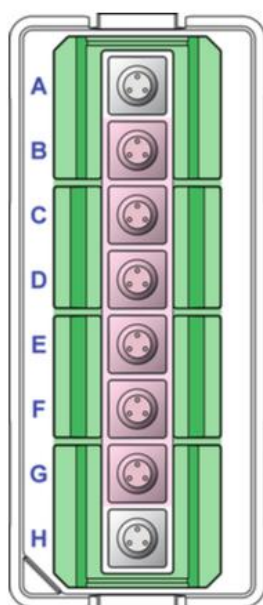


Figure 5 Seahorse XFp cell culture miniplate. Wells B, C and D were used for high glucose conditions with appropriate metformin treatment and E, F and G were used for the low glucose conditions with metformin treatments. Wells A and H were used for control without cells. Image taken from the Millipore Seahorse protocol²⁶.

Figure 5 is the layout of the seahorse miniplates, and highlighted in pink are the wells used for the treatments, the layout is the same for mito stress tests and glyco stress tests performed and 3 wells were used for each treatment of glucose and metformin concentrations. 24 hours after the cells were seeded the cells had attached, the media removed and appropriate glucose and metformin concentrations were added to the wells. The plates were then incubated for 48 hours before being analysed on the seahorse XFp analyser. 24 hours before analysis, the seahorse sensor cartridges was hydrated using water by putting 200µl of water into each

chamber and 400µl of water in the outside chambers. This was then incubated at 37°C overnight. Seahorse basal media was prepared using Seahorse XF DMEM Medium, pH 7.4 with added supplements of Seahorse XF L-Glutamine (200 mM solution), Seahorse XF Pyruvate (100 mM solution) and Seahorse XF Glucose (1.0 M solution). This basal stock was used for all mito and glyco stress tests, with additional supplements added based on which assay was being performed. 7.238ml of the basal media was put into a 15ml tube and labelled for MST experimental media. 7.425ml of the basal media was added to a 15ml tube and labelled GST experimental media, the MST tube had 75µl of glut and 187µl of 1M glucose added. The GST had 75µl added and glucose was not added as this was added during analysis to test how the cells reacted when glucose was introduced. Further the experimental media was then warmed to 37°C. The plates were then washed once with their respective new experimental media, removed and then 180µl added to all 8 wells ready for analysis, the plates were incubated for 45 minutes at 37°C. The cartridge, which was hydrated the day before, is removed and the compounds that are to be injected during the analysis were added.

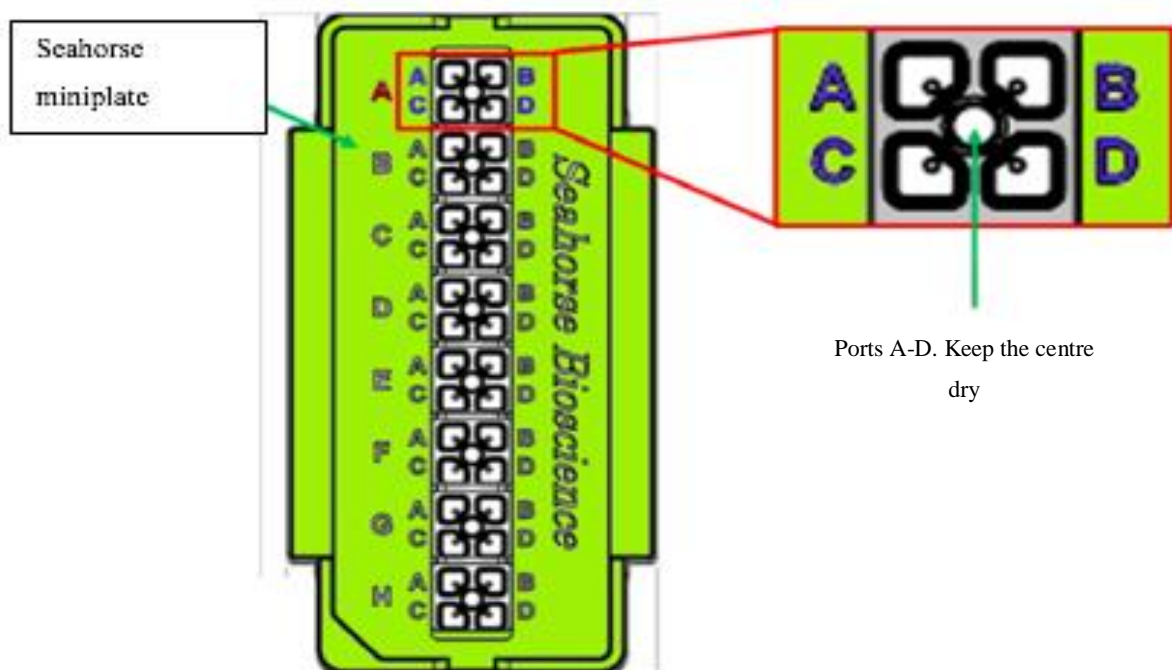


Figure 6 Seahorse XFp flux cartridge layout. Ports A-D for drugs to be introduced into the analysis. Image taken from the Millipore Seahorse protocol ²⁶.

The MTS and GST required different injections during analysis and also amounts of each were to be correctly added into the injector ports carefully. The compounds were taken out of the freezer were stock solutions and each needed diluting to the correct concentration in an Eppendorf tube. Table 1 contains the concentrations and dilution factors required for each test.

Table 2 List of compounds to be added to the mito stress and glycolysis stress test with dilutions amounts and how much to be added to each port on the Seahorse plate. *2-DG is added directly from the 1M stock

	Solutions to be injected	Port	Amount of media	Stock 2.5mM	Amount to add to the port
Mito Stress test	Oligomycin	A	247µl	3µl	22µl
	CCCP	B	999µl	1µl	20µl
	Rotenone	C	249µl	1µl	25µl
	Antimycin A	D	249µl	1µl	27µl
Glycolysis stress test	Glucose	A	242µl	8µl	25µl
	Oligomycin	B	247µl	3µl	25µl
	CCCP	C	999µl	1µl	25µl
	2-DG*	D	-	Stock 1M	25µl

After 45minutes of the Seahorse mini plate being incubated and all compounds were added, the flux cartridge was added with compounds into the seahorse analyser for optimization. When optimisation was complete, the cartridge was release from the seahorse and was exchanged for the cell culture mini plate with cells in seahorse basal media, and the analysis begun after inputting the setting for the analysis into the machine. The plate settings were to instruct the seahorse as to which cell conditions were in each well of the miniplate and which compounds were to be injected and in what order. When the analysis was finished the plate was removed and cells were removed and the plate was prepared for bicinchoninic acid assay (BCA). The BCA was performed using Pierce™ BCA Protein Assay Kit to determine the total concentration of protein in each sample, the absorbance was read on the Molecular Devices Spectramax Paradigm at a wavelength of 562nm. Using the standard curve created,

the amounts of protein (μg) in each sample were used to normalise the seahorse data on the Seahorse Wave 2.6.0 Software.

3.5 BrdU Proliferation Assay

The assay was performed using Millipore BrdU Cell Proliferation Assay using antibodies to detect bromodeoxyuridine(BrdU), which is synthesized into the DNA of a cell as a replacement for 3H thymidine.

This assay was performed twice using cell lines SW948 and SW1116 the first assay using SW948 p20 and SW1116 p14 with 5000 cells seeded in each well. The second assay using SW948 p22 and SW1116 p17 with 10000 cells seeding in each well. Cells were seeded in a Corning black coated 96 well plate using 100 μl with 17 wells used for each high and low glucose concentrations of each cell line, which consisted of 3 replicates of 5 variables of metformin concentrations plus wells for negative controls containing no BrdU. 100 μl of the test reagent was added on top of the media and incubated for 28 hours. BrdU stock solution was diluted 1:500 and 20 μl was added to the wells in which were to be labelled and incubated for a further 20 hours and then the media removed and 200 μl of the stock fixing solution added to each well for 30minutes at room temperature, then removed. The stock washing buffer was diluted 1:50 using distilled water and used to wash the plate 3 times, in which after the plate is blotted dry. 100 μl of the provided detector antibody was added to each well and incubated for 1hour at room temperature and then the washing steps repeated. The goat anti-mouse IgG peroxidase conjugate stock was diluted 1:2000 using conjugate dilute and filtered using a 0.22 μm syringe. 100 μl of the antibody was added to each well and incubated at room temperature for 30 minutes, then wash step is repeated for a third time. 100 μl of the TMB peroxidase substrate was added to each well and incubated for 30 minutes at room temperature in the dark. 100 μl of the provided stop solution is added to each well and then the absorbance was read on the Molecular Devices Spectramax Paradigm plate reader at dual wavelength 450/595. The plate was shaken for 15 seconds before it was read and the optimization was performed before reading.

3.6 Alamar Blue Assay

The assay was performed four times; SW948 at passage numbers p20, p22, p24 and p26 and SW1116 at passage numbers p20, p21, p23 and p24. 3500 cells were seeded into each well using Corning black coated 96 well plates with clear bottoms with five wells used for each variable, a plate was made for analysis after 24 hours and 48 hours. Each SW948 and SW1116 were tested in high and low glucose concentrations, with metformin concentrations of 0mM (control), 0.5mM, 1.0mM, 3.0mM, 5.0mM and 10.0mM. A 96-well plate was used for each cell line. Each well was seeded with 3500 cells in 200µl of high glucose media to allow the cells to attach to the plate. After 24 hours, the media was removed and 200µl of media with appropriate concentrations of glucose and metformin was added. Using the Alamar Blue kit from Biosciences a 1:10 dilution was made from 4,84mM to 484µM in PBS, and 20µl was added to each well 4 hours before the 96well plate was to be analysed, this gave a final concentration of 44µM of Alamar Blue in each well. At 24 and 48 hours, the plates were analysed using the Molecular Devices Spectramax Paradigm plate reader. The settings were set to read fluorescence at wavelengths of 530nm and 590nm, the plate was shook for 15 seconds before reading and the plate optimization was performed.

Table 3 Conditions used for Alamar Blue, each low glucose and high glucose concentration was tested with five concentrations of metformin (0.5mM, 1.0mM, 3.0mM, 5.0mM 10.0mM) and a control with no metformin

Cell lines	SW948			SW1116		
Glucose concentrations	High 4.5g/L (5mM)			Low 1g/L (25mM)		
Metformin concentrations	Control 0.0mM	0.5mM	1.0mM	3.0mM	5.0mM	10.0mM
Controls	No cells with treatment and Alamar Blue			Cells seeded with treatment without Alamar Blue		

3.7 Immunocytochemistry: Confocal Imaging of OCT1

Immunocytochemistry (ICC) was performed using cell line SW948 at passage numbers p13 and p24 and cell line SW1116 at passage numbers p13 and p20.

3.7.1 Seeding

10,000 cells of SW948 and 20,000 cells of SW948 were seeded in 200µl of high glucose media into Ibidi µ-Slide 8 Well plates and left 24 hours to attach. The media was removed and new experimental media was added with one well for each metformin concentration of 0.0mM (control), 0.5mM and 3.0mM for both high and low glucose. The final two wells were used for a negative control in which primary antibody was not added. A plate was prepared for each for 6 hours, 12 hours, 24 hours and 48 hours. The experimental media was added at the same time and after each time period, the media was removed and the cells were fixed by adding 150µl of 4% paraformaldehyde (PFA) for 30 minutes at room temperature. The PFA was removed and PBS was added, and stored at 4°C until staining.

3.7.2 Staining

Cells were washed with PBS twice and then 200µl of blocking buffer (BB) made up of a ratio of 7 parts dH₂O, 2 parts FCS and 1 part PBS-Tween 0.2% was added to each well for 1 hour at room temperature and then removed. Primary antibody (AB) *SLC22A1* (OCT1) was diluted in blocking buffer at 1:200 (AB:BB) and 100µl was added to each well and incubated overnight at 4°C (Not added to the negative control). The next day, after removing the primary AB, the wells were washed 4x with PBS for 5 minutes each wash. The secondary AB was diluted in the BB at a ratio of 1:500. The secondary antibody used was a Goat Anti-Mouse Alexa Fluor 568 (the primary was mouse) and 100µl was added to each well and incubated at room temperature away from direct light for 1 hour. After removing the secondary AB, 100µl of Hoeschst 33342 diluted 1:1000 (2µl/ml) was added to each well for

3 minutes and then quickly removed. Each well was then washed 4 times with PBS for 5 minutes each wash. PBS was added to each well to ensure the cells do not dry.

3.7.3 Imaging

The plates were imaged using the Leica TCS SP8 CSU Confocal Microscope 20x objective and images were analysed using the Leica LASX Software for windows.

Two channels were used; the image channel properties for each were:

Hoechst - Blue channel, laser intensity at 2.5

Alexa 568 – Yellow channel, laser intensity 2.8

To ensure an un-bias analysis of the images, protocols were implemented to follow when selecting data. The images were quantified using a ratio of staining; OCT-1:Hoeschst. This was to assess if the amount of OCT-1 changes depending on concentration of glucose and metformin, and also between two colorectal cancer cell lines SW948 and SW1116.

A layout of 5 regions of interest (ROI) were used, and an average of the 5 were taken for comparison. Although the ROI's were assigned without bias, each had to be the same size in comparison to the pixel size of the image, it was attempted to have at least 3 ROI's containing both blue and yellow staining, and follow the same layout. The 5 ROI's followed the following layout

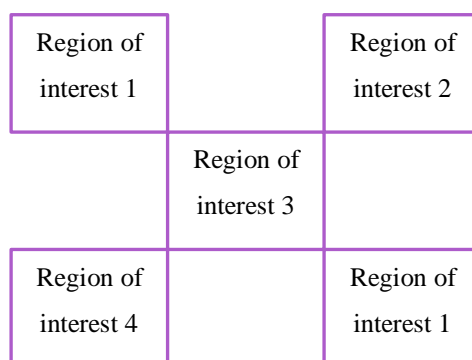


Figure 7 Layout of the five region of interest's used to quantify data in LASX of the ratio of OCT1:Hoeschst from the images taken on the Leica TCS Confocal Microscope using the 20x objective

If not all 5 ROIs contained both blue and yellow staining then 3 ROI will were used at best fit. If the correct number of cells were not achieved then an image that gives 3 ROI data was used and the cells were imaged with and without the ROI's to show the location of the data collected. Images were taken using the 60x objective to give clearer images of OCT1 location.

4 Results

4.1 Growth Of SW948 And SW1116

4.1.1 SW948 Proliferates Quicker Than SW1116

SW948 are glycolytic and require glycolysis to get their energy. SW948 quickly use the glucose in the media to create a lactate rich environment, this is evident in the yellow colour of the media after several days in the incubator.

SW1116 are not as glucose dependant and favour getting their energy from the mitochondria of the cell using OXPHOS.

Observing cell growth over 72 hours shows that the SW948 cells replicate at a much faster rate than SW1116.

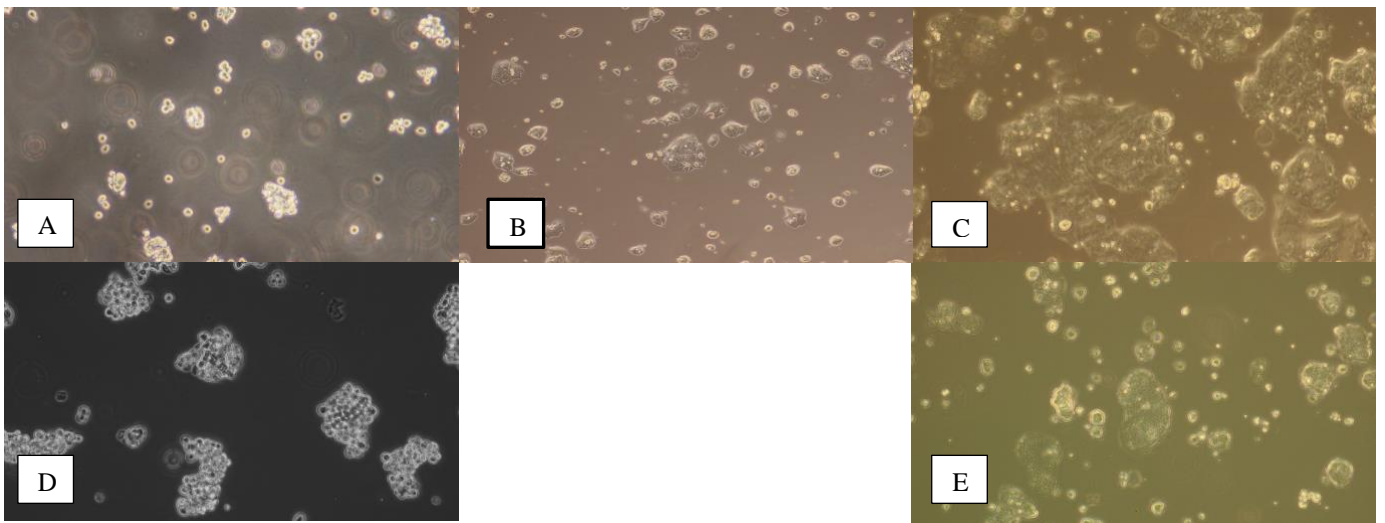


Figure 8 Images of cells lines SW948 and SW1116 showing growth differences. (A) SW948 2 hours after passaging, (B) SW948 24 hours, (C) SW948 48 hours, (D) SW1116 2 hours after passaging, (E) SW1116 48 hours after passaging .

Images taken of SW1116 after 24 hours gave a similar picture and often were lower in numbers than the seeded amount.

The doubling time for each cell line was assessed at high glucose concentrations (25mM) versus low physiological glucose concentration (5mM) to assess how the cells proliferate

under different concentrations of glucose. Doubling time is calculated to give an indication as to how long it takes for a numbers of cells to double.

SW948 takes 28 hours in high glucose and 25 hours in low glucose. SW1116 takes 63 hours in high glucose and 50 hours in low glucose. This is using the growth of the cells after 72 hours.

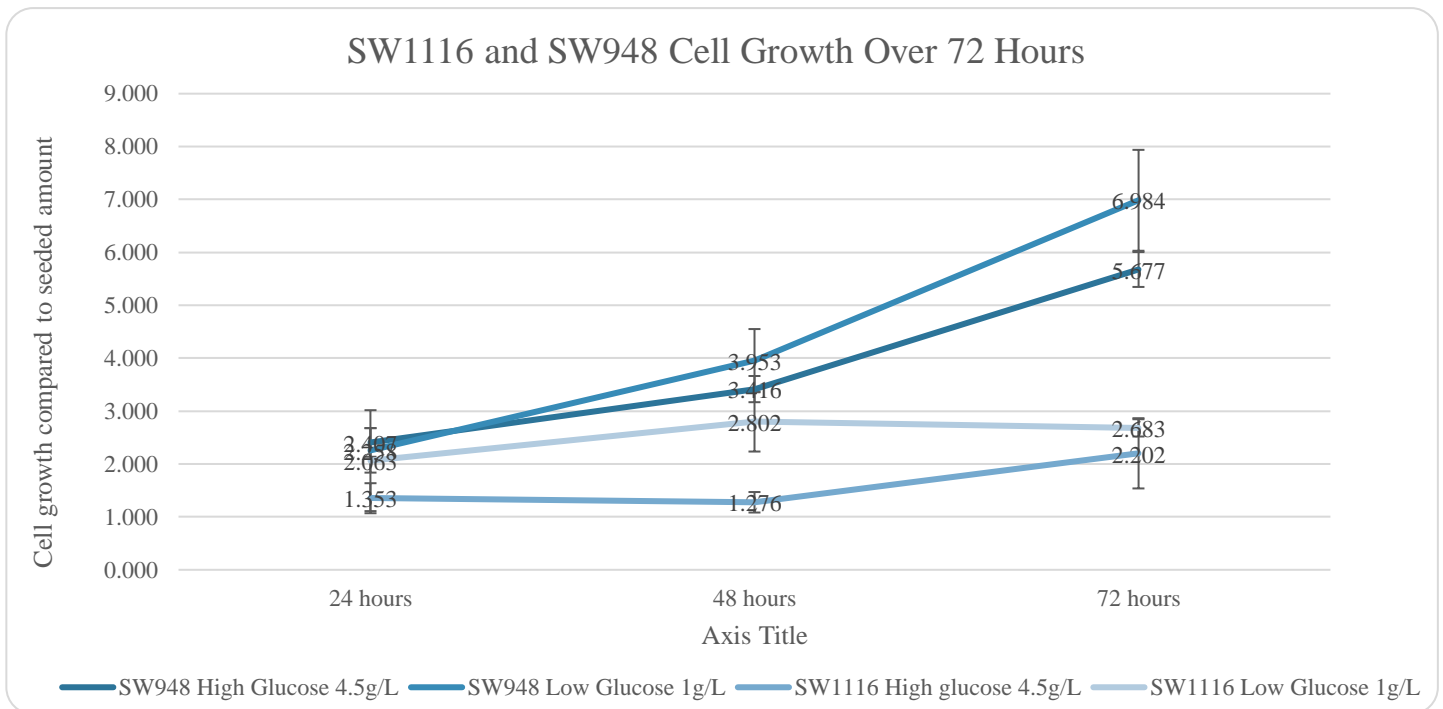


Figure 9 - Cell growth of SW1116 & SW948 over 72 hours based on initial seeding of 100,000 cells of SW948 and 200,000 of SW1116.

Figure 6 contains growth of the cells over 72 hours and indicates that in cell lines SW948 and SW1116 the concentration of glucose has an effect on the growth of the cells. In SW948 there was a 7-fold increase in cells from initial seeding in the physiological low glucose and 5.6 fold in high glucose. SW1116 had a similar trend in that the low glucose with 2.6 times increase proliferated quicker than the high glucose with a 2.2 increase over 72 hours. It is also clear to see that SW1116 in high glucose found it harder to proliferate in the earlier stages of the test.

After 72 hours of growth using the high and low glucose values from figure 6 the SW948 is

proven to be statistically different between the two concentrations of glucose ($t=0.00038$, $p=0.046$). SW1116 is also proven to be statistically different ($t=0.022$, $p=0.022$).

4.2 Glucose Concentrations have an effect on the Metabolic Phenotype of Colorectal Cancer Cells Lines SW948 and SW1116

Mitochondrial respiration was analysed using the mito stress test (MST) and also how well the cells used glucose and the pathways for glycolysis using the glycolysis/glyco stress test (GST). Each of the stress tests compared ECAR (glycolytic activity) vs OCAR (mitochondrial respiration) to produce the results. SW948 gives results of a more glycolytic and energetic profile, and does differ between high and low glucose concentrations (Fig 10, 11). For SW1116, the graphs indicate that the cells have a more aerobic profile and that prefer to use the mitochondria for energy. The images also show that the lower the glucose concentration in SW1116 the more aerobic the cells become (fig 12, 13)

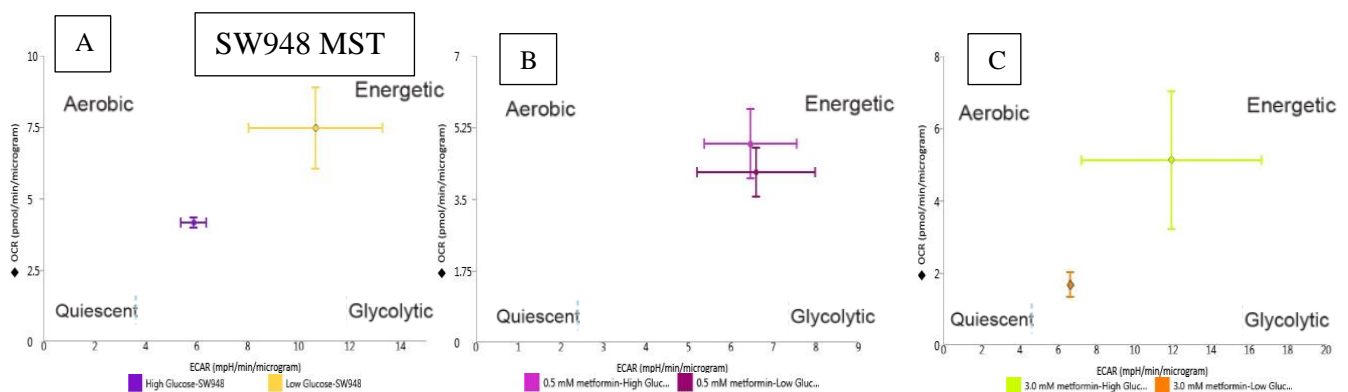


Figure 10 Wave 2.6.0 results from the seahorse XFp analyser. Mito stress test on colorectal cancer cell line SW948 in high glucose and low glucose concentrations under three different treatments of metformin. (A) Control with no metformin, (B) 0.5mM of metformin, (C) 3.0mM of metformin. The graphs represent OCR vs. ECAR normalised using micrograms of protein present in the samples.

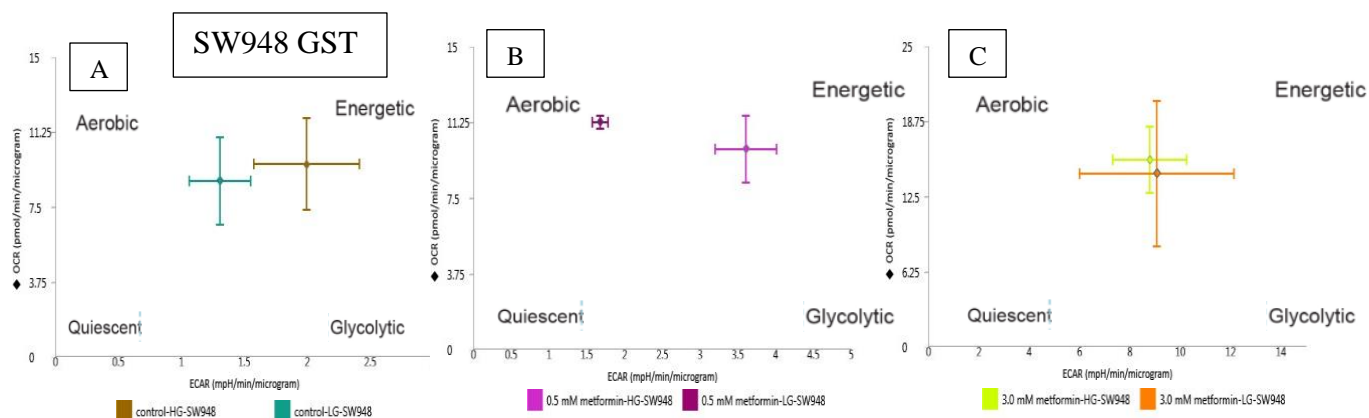


Figure 11 Wave 2.6.0 results from the seahorse XFp analyser. Glycolysis stress test on colorectal cancer cell line SW948 in high glucose and low glucose concentrations under three different treatments of metformin. (A) Control with no metformin, (B) 0.5mM of metformin, (C) 3.0mM of metformin. The graphs represent OCR vs. ECAR normalised using micrograms of protein present in the samples.

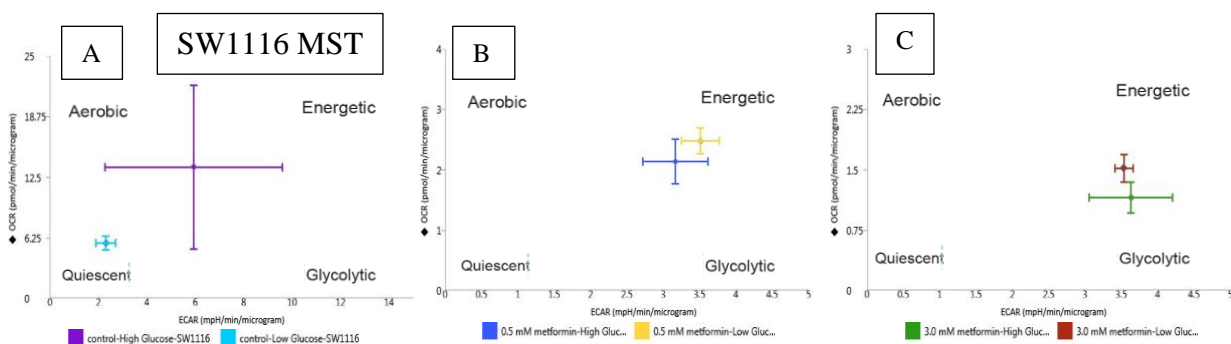


Figure 12 Wave 2.6.0 results from the seahorse XFp analyser. Mito stress test on colorectal cancer cell line SW1116 in high glucose and low glucose concentrations under three different treatments of metformin. (A) Control with no metformin, (B) 0.5mM of metformin, (C) 3.0mM of metformin. The graphs represent OCR vs. ECAR normalised using micrograms of protein present in the samples

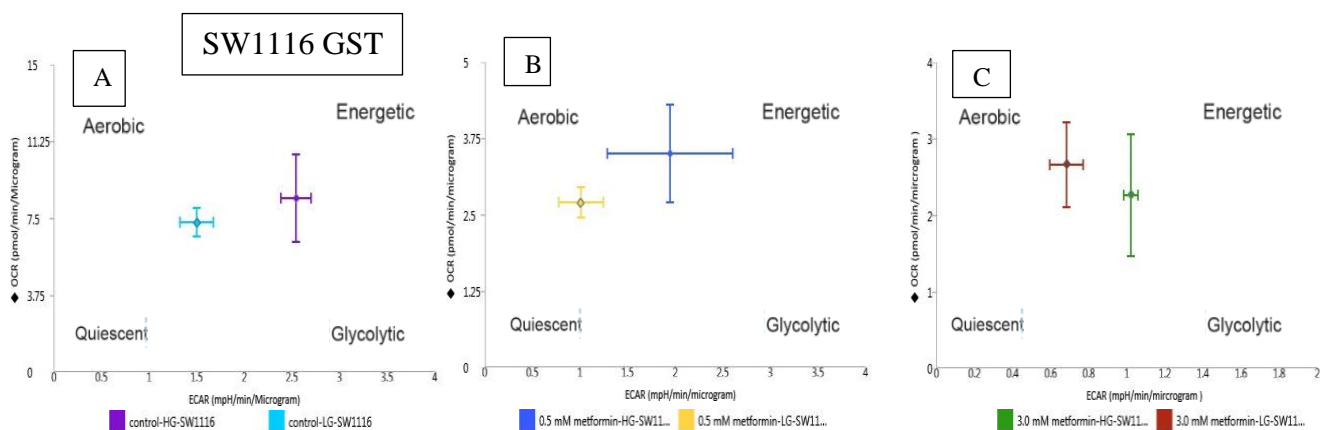


Figure 13 Wave 2.6.0 results from the seahorse XFp analyser. Glycolysis stress test on colorectal cancer cell line SW1116 in high glucose and low glucose concentrations under three different treatments of metformin. (A) Control with no metformin, (B) 0.5mM of metformin, (C) 3.0mM of metformin. The graphs represent OCR vs. ECAR normalised using micrograms of protein present in the samples

4.3 Increase in Concentrations of Metformin Inhibit Colorectal Cancer Cell Growth

Proliferation and viability assays were both performed using absorbance and fluorescence reading on the spectramax plate reader to assay cell growth under various concentrations of metformin, to assess the affect and also to determine metformin concentrations suitable for future testing.

4.3.1 Brdu Proliferation Assay

This assay detects 5-bromo-2'-deoxyuridine (BrdU) which is in the cell's DNA. This is a pyrimidine that replaces the thymidine in regular cell growth. An antibody for BrdU is added which allows for fluorescence to be analysed²⁷. This is used for the purpose of comparing fluorescence values given to compare changes in growth depending on concentration of metformin being added. Analysis of both SW1116 and SW948 in high and low glucose showed that growth of the cells were effects by increasing concentrations of metformin.

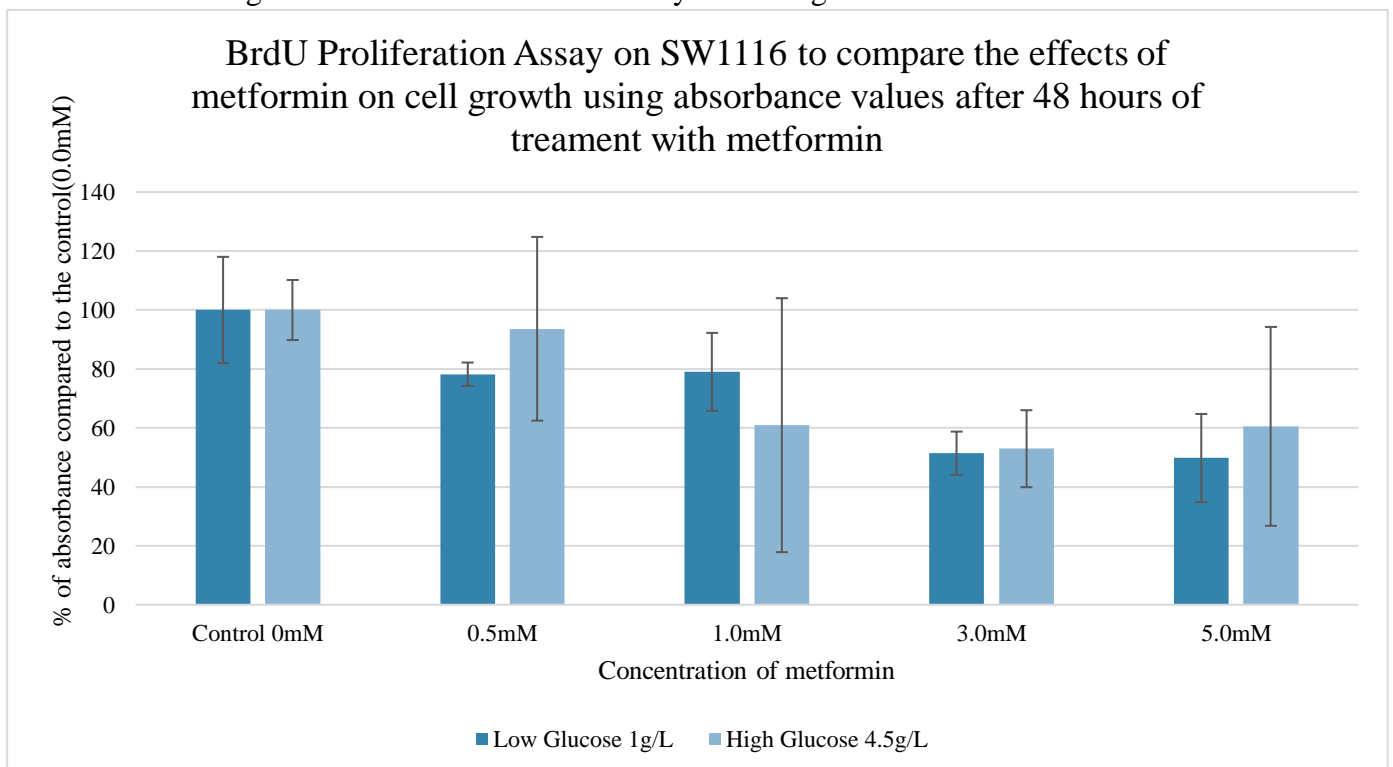


Figure 14 Results from BrdU proliferation assay on colorectal cancer cell line SW1116. Each result for the respective metformin treatment is compared against the control for each high glucose and low glucose concentrations using the absorbance read on the spectramax plate reader

In high and low glucose, 3.0mM of metformin induced a 50% reduction in cell numbers for SW1116 (Fig. 14) and almost the same decrease for both glucose concentrations for SW948 (Fig. 15). High glucose for both cell lines declined at a consist rate for all metformin concentration, and although the low glucose samples was not as consistent it did also decrease the numbers of cells for both cell lines with increase of metformin concentration.

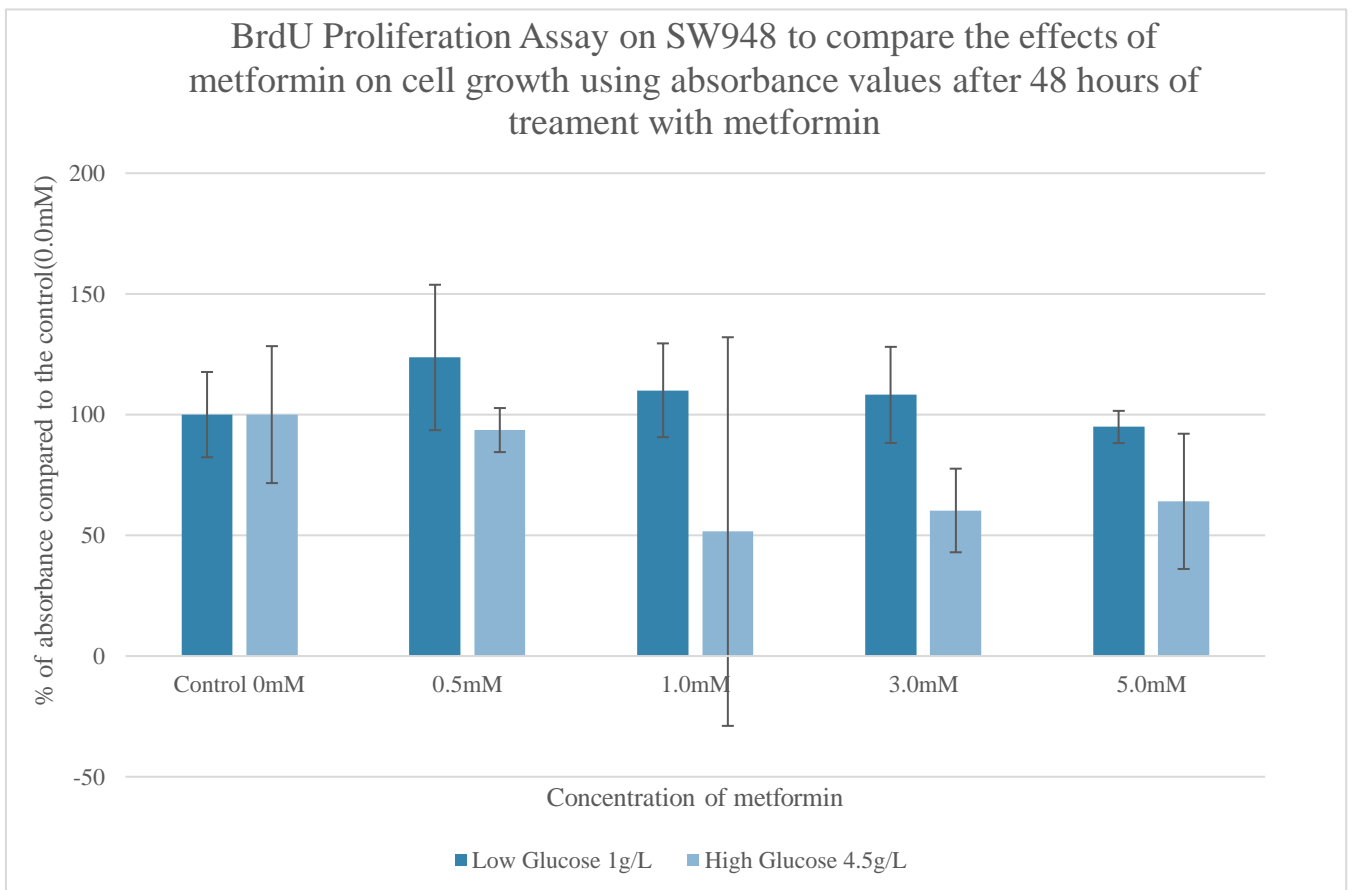


Figure 15 Results from BrdU proliferation assay on colorectal cancer cell line SW948. Each result for the respective metformin treatment is compared against the control for each high glucose and low glucose concentrations using the absorbance read on the spectramax plate reader.

4.3.2 Alamar Blue Viability Assay

Alamar blue is a viability assay, the process analysed is the reduction of resazurin to resorufin.²⁸ Resazurin is mostly non-fluorescent but it is the reduced form of resorufin which provides the fluorescence to be analysed.

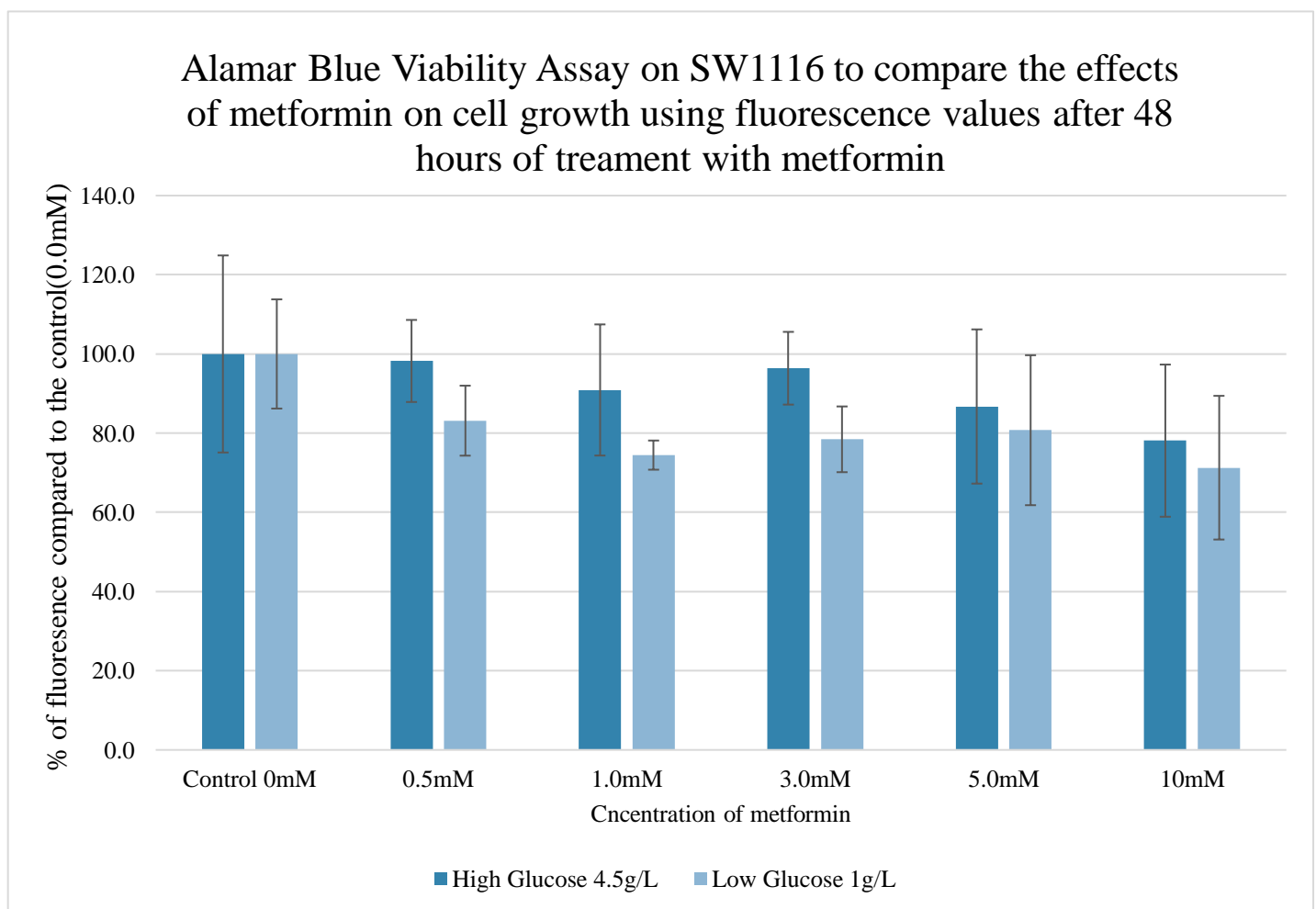


Figure 16 Results from alamar blue viability assay on colorectal cancer cell line SW1116. Each result for the respective metformin treatment is compared against the control for each high glucose and low glucose concentrations using the fluorescence read on the Spectramax plate reader

Figure 16 above, of SW1116 fluorescence values, show that when metformin concentrations are increased the cell number decreases. Though changes are not huge it does show that with increased amounts of metformin there is a repression of cell replication. In a low glucose treatment, it demonstrates that the increase in metformin concentration has a larger effect when metformin increased.

SW948 fluorescence results shown in figure 17 have clear difference when metformin is present compared to a control sample. This is the case for both high and low glucose

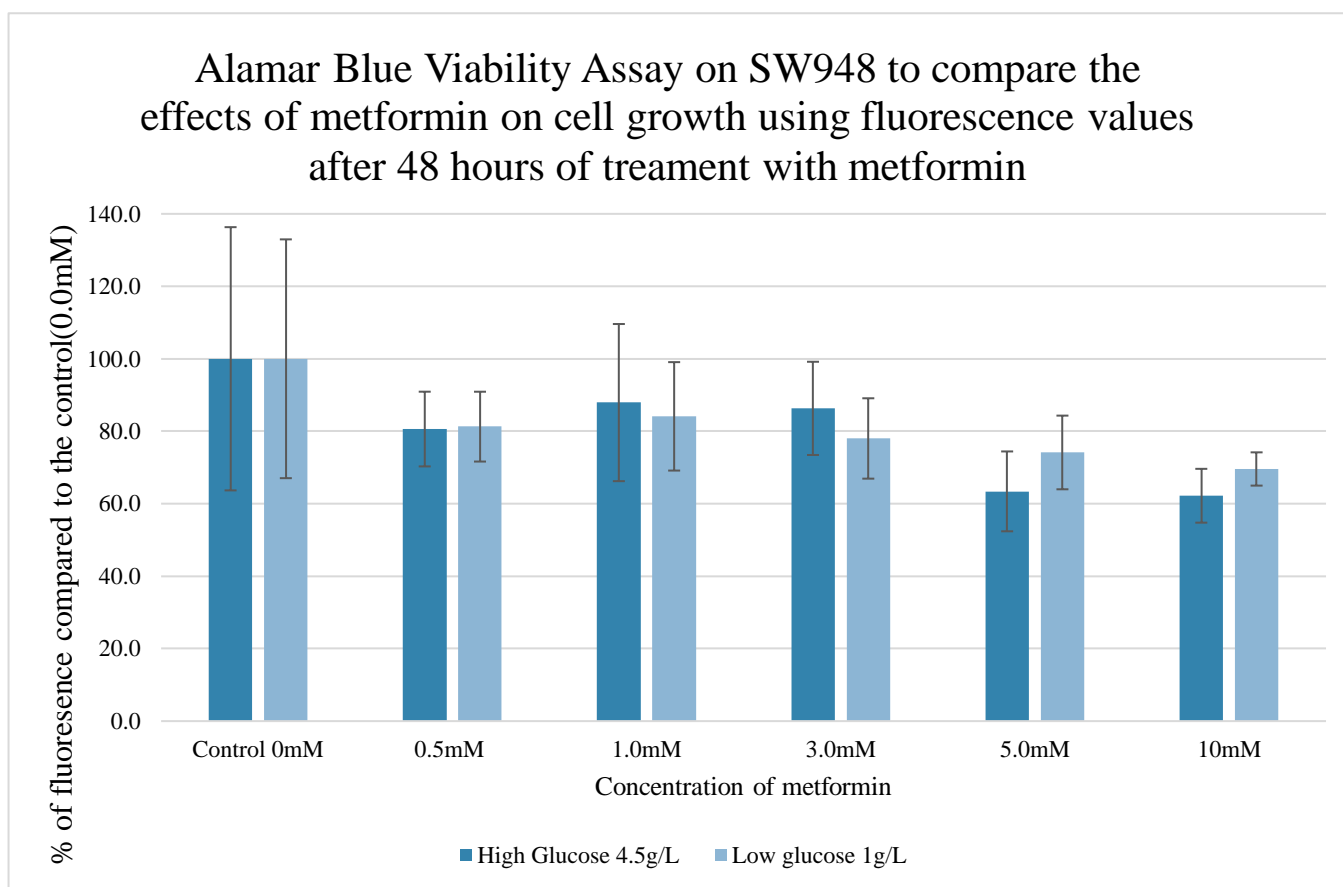


Figure 17 Results from alamar blue viability assay on colorectal cancer cell line SW948. Each result for the respective metformin treatment is compared against the control for each high glucose and low glucose concentrations using the fluorescence read on the Spectramax plate reader

concentrations. This would suggest that as the metformin concentration increases, there are less cells in the well, and that metformin does have an effect on cell growth. From the analysis of results for both SW1116 and SW948, the concentrations 0.5mM and 3.0 were used for future experiments on the cells. This is because they had a clear difference in cell numbers over the spread of both cells lines results for both viability and proliferation assays.

4.4 OCT1 Responsible for Transporting Metformin Is Located on the Outside of the Cell

To image the location of OCT1 immunocytochemistry was performed and cell lines SW948 and SW1116 were stained for imaging on the Leica Confocal Microscope and analysed using Leica LASX software. OCT1 is responsible for transporting metformin across the cell membrane into the cell, where it reaches the mitochondria.

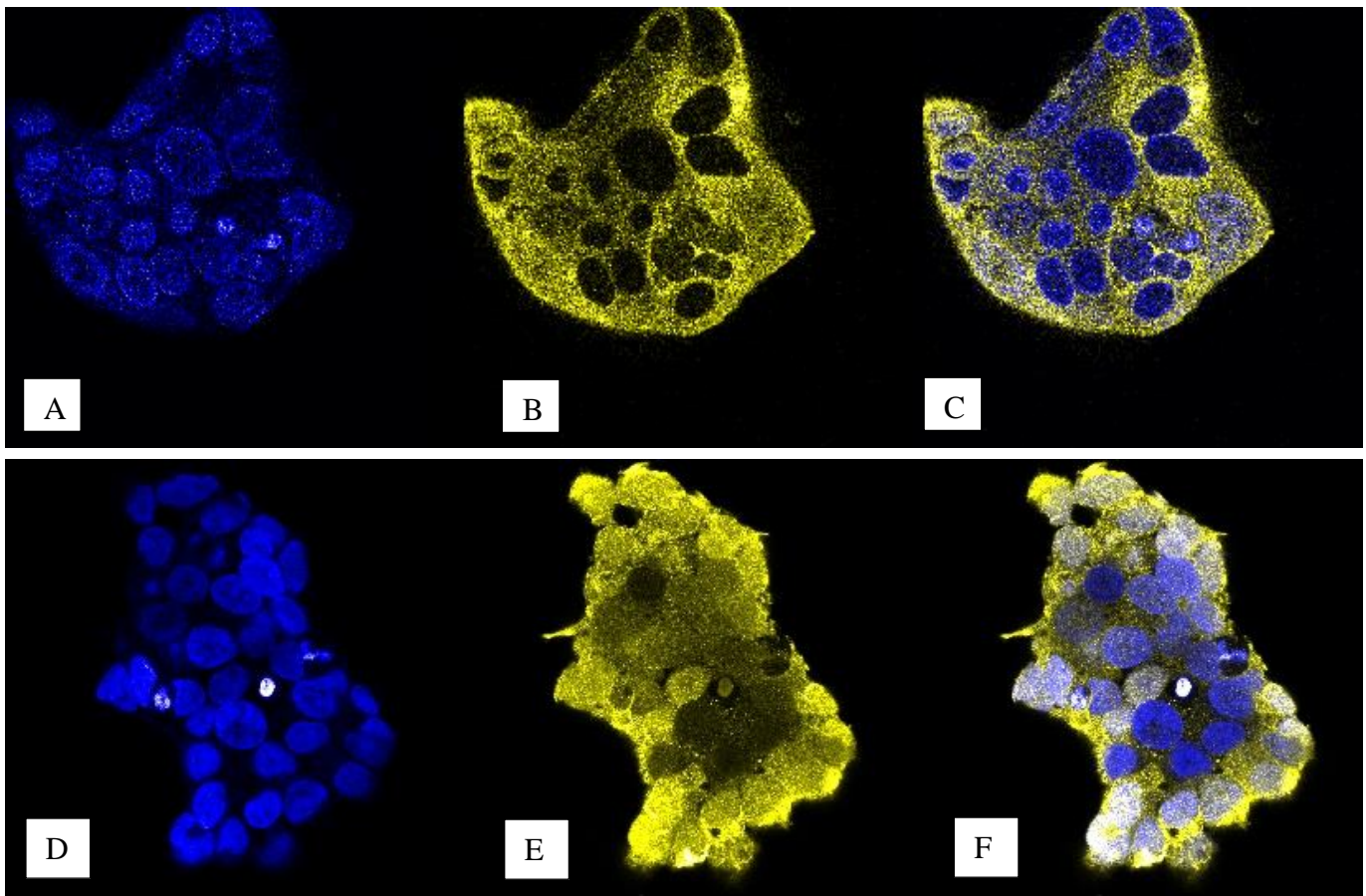


Figure 18 Images of the location of OCT1 in yellow to the nucleus in blue, images were analysed on the Leica LASX to show location of OCT1. (A-C) SW1116 High Glucose control sample after 48 hours, showing staining of the nucleus in blue, staining of OCT1 in yellow and overlap of both stains together (D-F) SW1116 High Glucose with 0.5mM metformin treatment after 48 hours showing staining of the nucleus with hoeschst in blue, staining of OCT1 in yellow and overlap of both stains together. Images were taken on the Leica Confocal imaging microscope with the 63x objective. The nucleus was stained using Hoechst and OCT1 with primary antibody *SLC22A1*. The cells were not permeabilised.

Figure 18 indicates that OCT1 presented in yellow is located on the outside of the cell, as the staining did not have a permeabilization step, the primary antibody for OCT1 was not intended to go inside the cell. Negative controls samples that did not have the primary

antibody were also imaged to eliminate any unspecific binding of the secondary antibody which would give a signal for the yellow channel in locations in which do not have OCT1.

The cells, when clumps formed, created a barrier in which either made it difficult for the antibody to enter and create a stain or decrease the expression of OCT1.

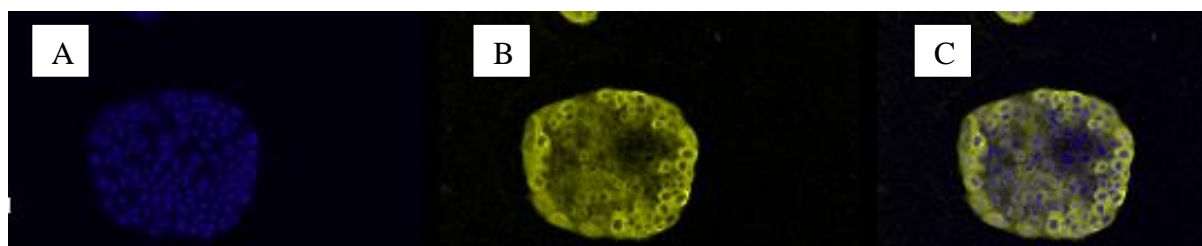


Figure 19 Image of sample taken for SW1116 Low Glucose 3.0mM after 48 hours. (A) Stained nucleus as blue (B) Stained OCT1 as yellow (C) Overlay of the images. Images were taken using 20x objective on the Leica Confocal Microscope.

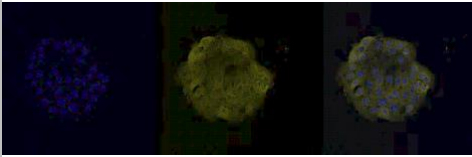
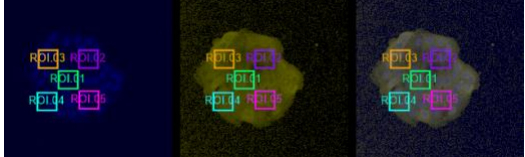
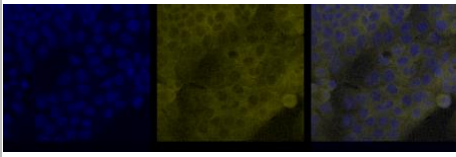
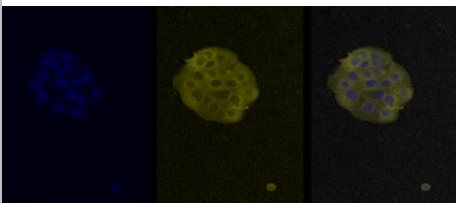
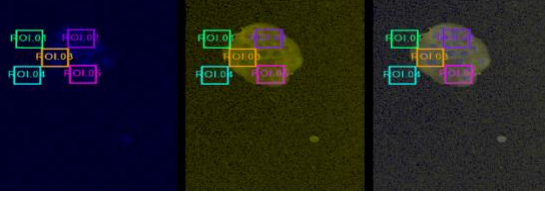
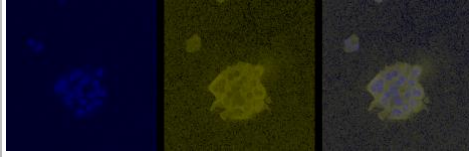
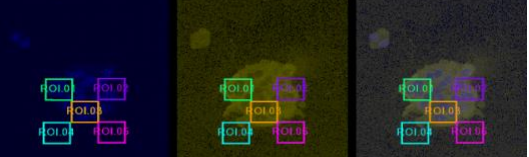
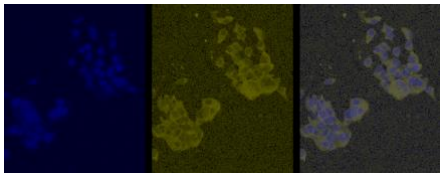
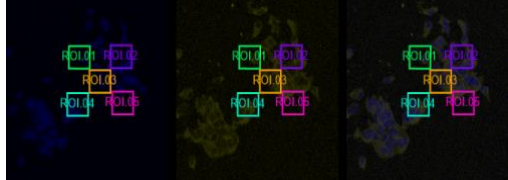
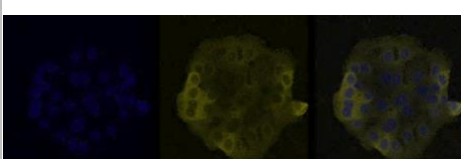
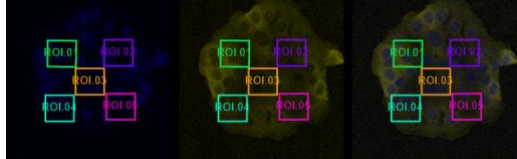
Figure 19 shows that image (A) has cells indicated by blue and that image (B) does not have an even distribution of the yellow stained as a relation to the amount of cells.

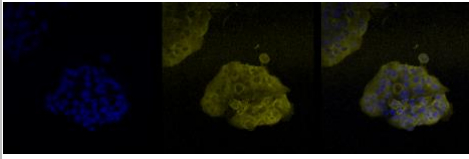
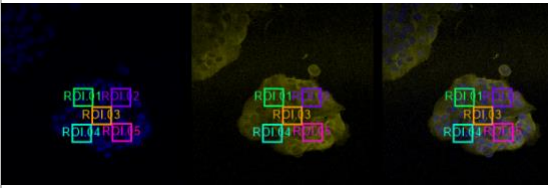
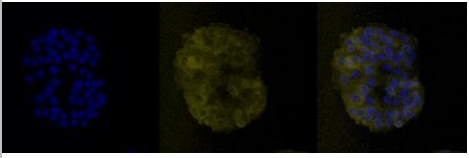
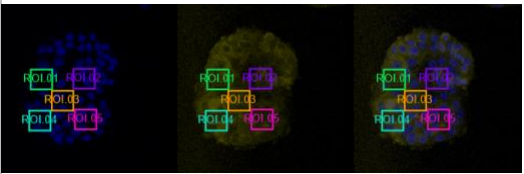
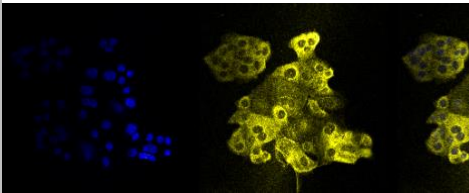
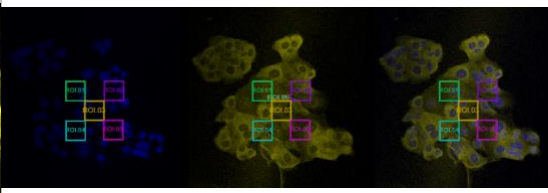
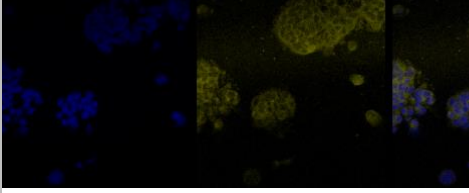
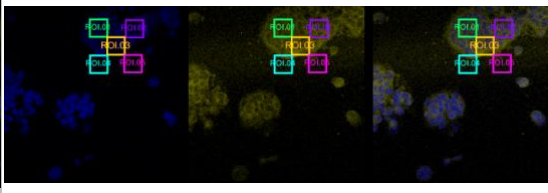
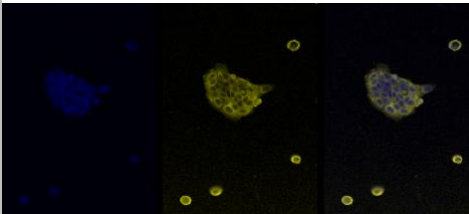
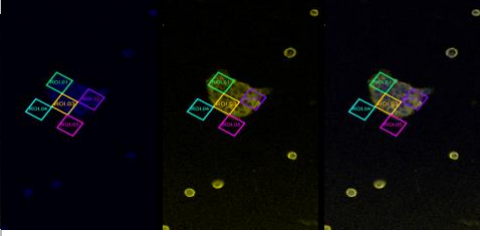
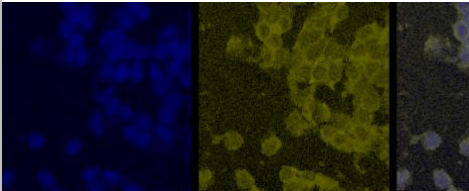
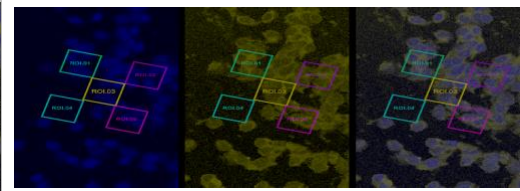
4.4.1 Confocal Imaging of OCT1

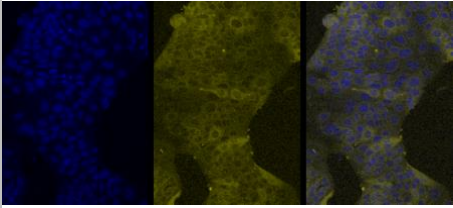
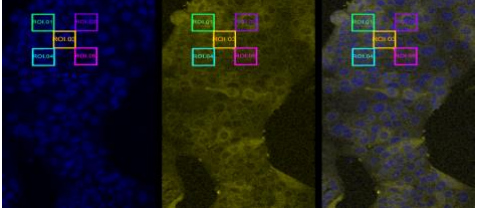
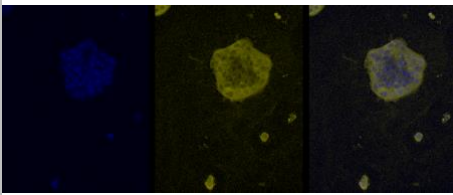
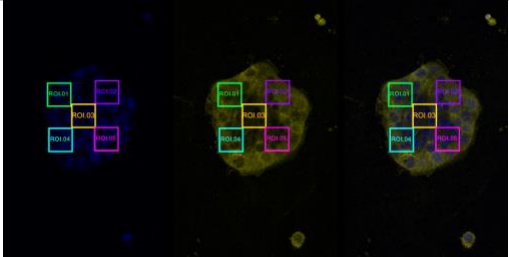
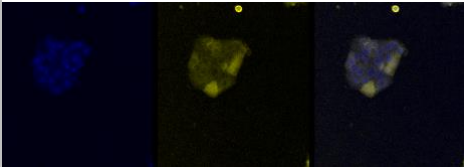
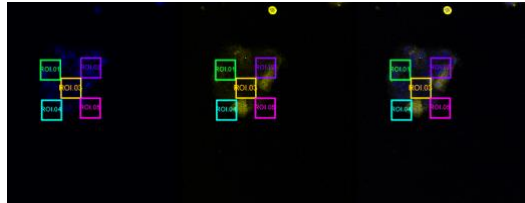
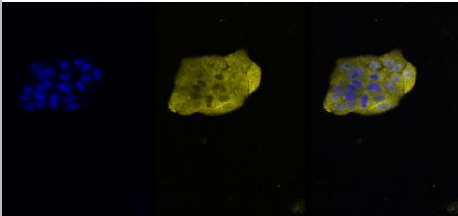
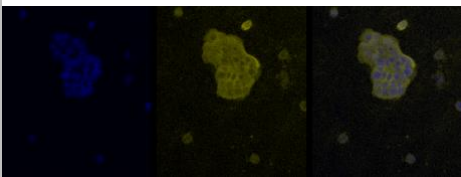
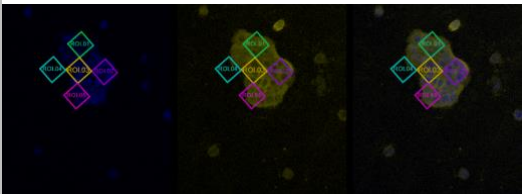

Colorectal cancer cell lines SW948 and SW1116 were stained and images using confocal imaging and analysed using the Leica LASX software, after taking images for identifying the location of OCT1, the images were not sufficient enough to assess if OCT1 expression changes based upon cell line, glucose concentrations or concentrations of metformin.

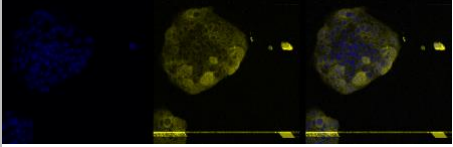
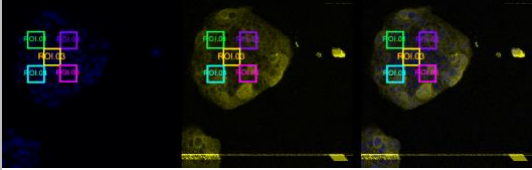
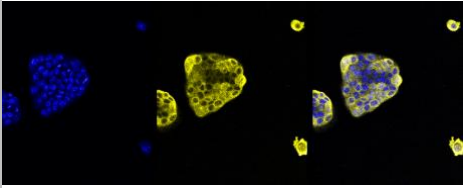
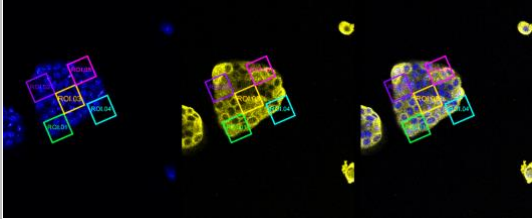
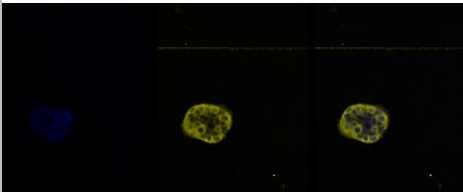
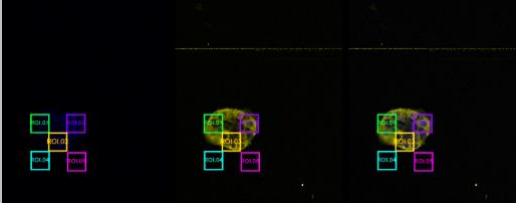
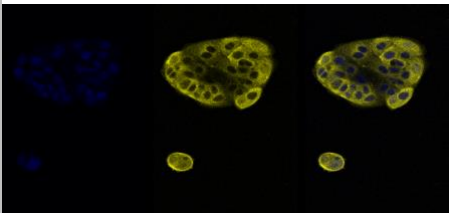
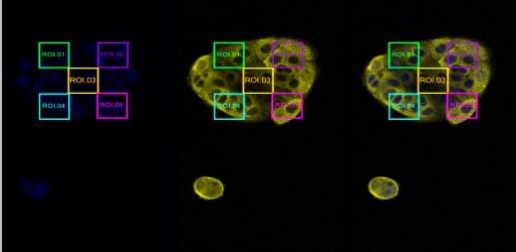
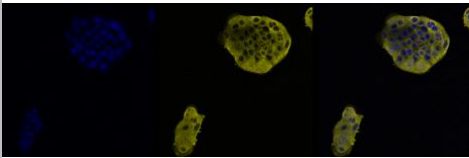
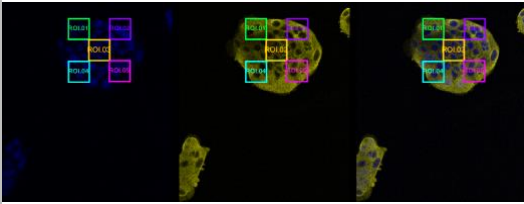
Therefore the images needed quantifying, to determine this the OCT1 and Nucleus grey scale ratio was calculated using 5 regions of interest (ROI). Each treatment has an image with and without the ROI to show which areas were taken for quantification. The ROI's stayed the same layout for every image to minimize any bias data.

Table 4 Images taken on the Leica Confocal Microscope after analysis using Leica Application Suite 2.0 to add regions of interest to collect data of OCT1 in yellow using antibody SLC22A compared to the nucleus in blue stained with hoeschst in colorectal cancer cell line SW948. The treatment conditions shown are 6 hours, 12 hours, 24 hours and 48 hours using high glucose labelled HG and low glucose labelled LG with metformin treatments of 0.5mM and 3.0mM including a control which was used to compare the changes in OCT1 using the regions of interest.

Treatment conditions			Without ROI	Added ROI
6 hours	HG	Control		
		0.5mM		
		0.3mM		
	LG	Control		
		0.5mM		
		0.3mM		

12 hours	HG	Control		
		0.5mM		
		0.3mM		
	LG	Control		
		0.5mM		
		0.3mM		

24 hours	HG	Control		
		0.5mM		
		0.3mM		
		Control		
	LG	0.5mM		
		Control		

		0.3mM		
48 hours	HG	Control		
		0.5mM		
		0.3mM		
		LG Control		

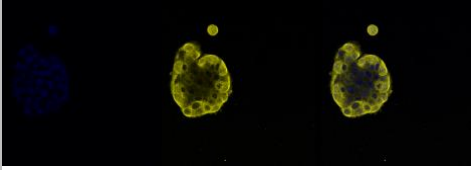
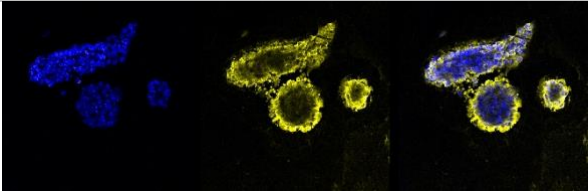
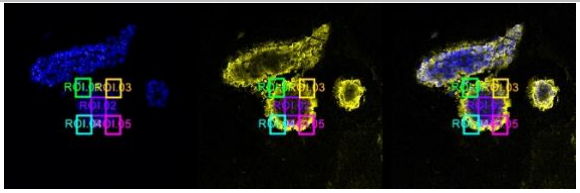
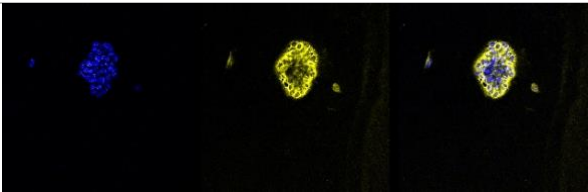
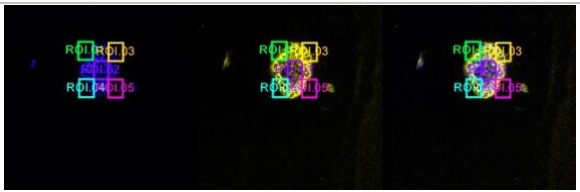
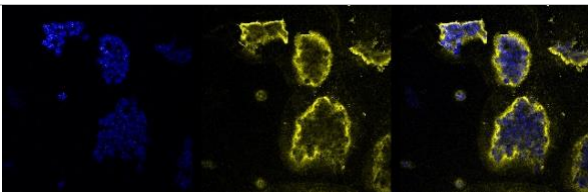
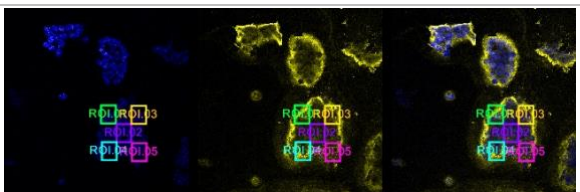
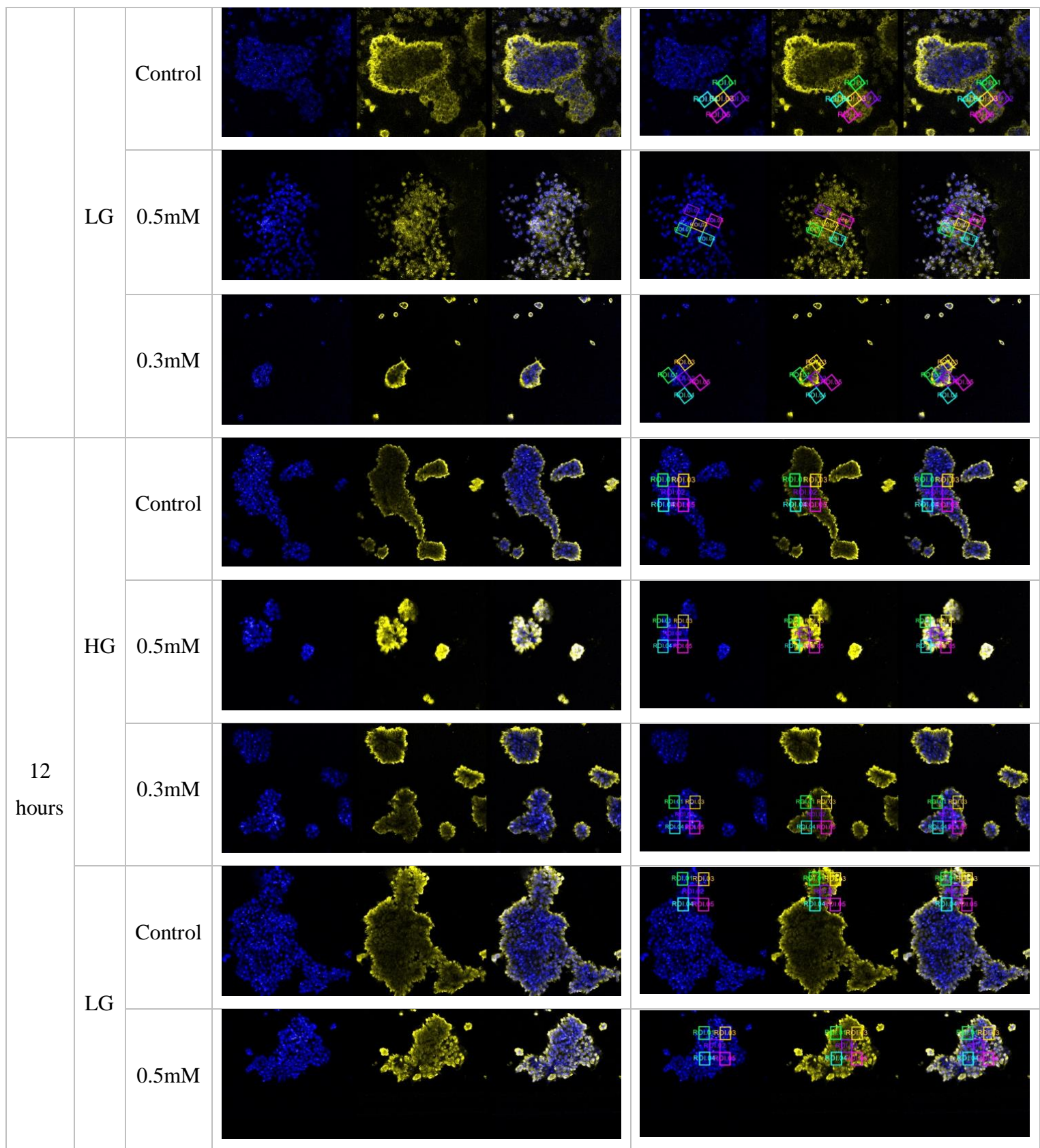
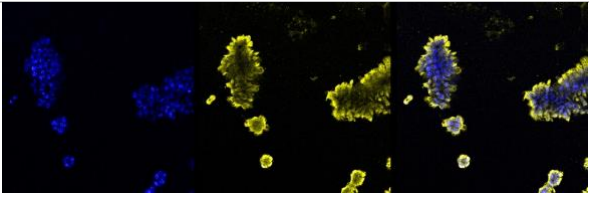
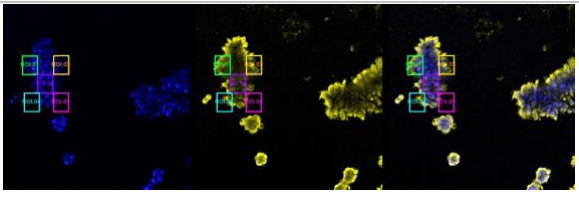
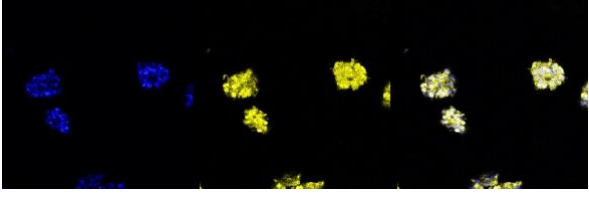
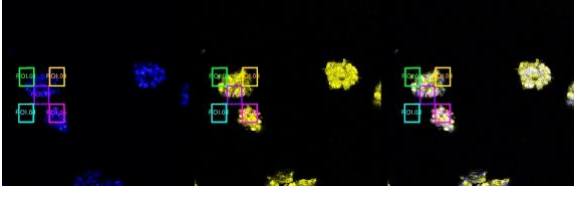
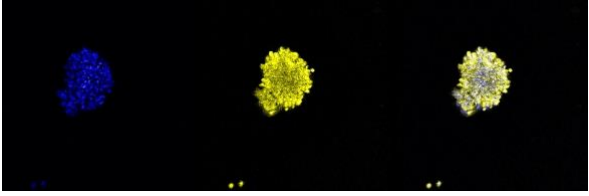
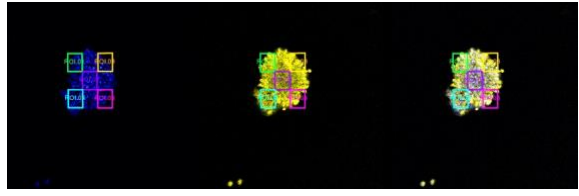
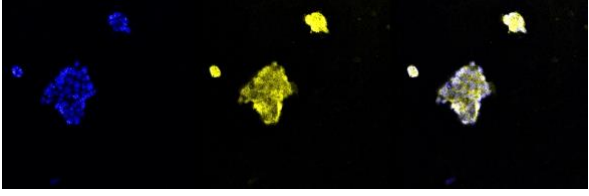
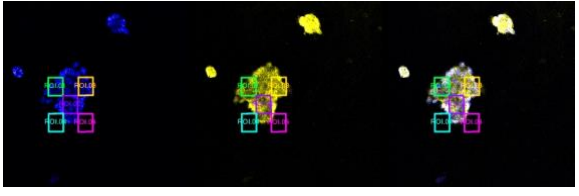
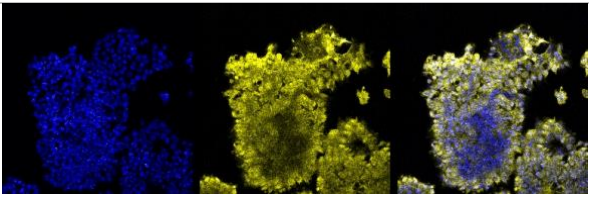
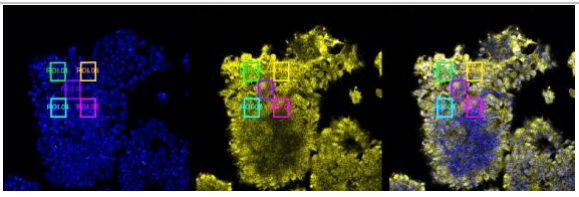
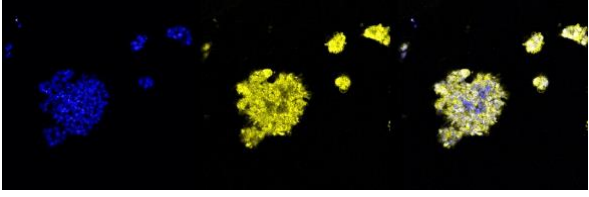
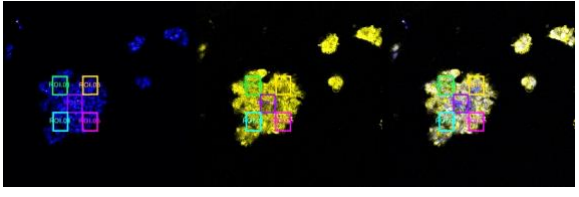
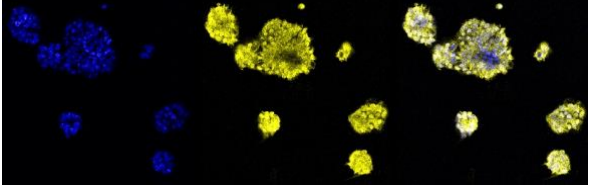
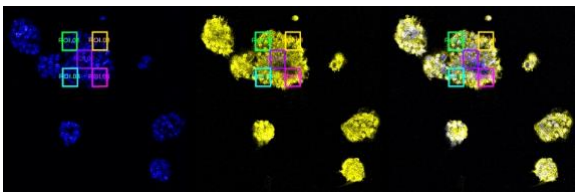
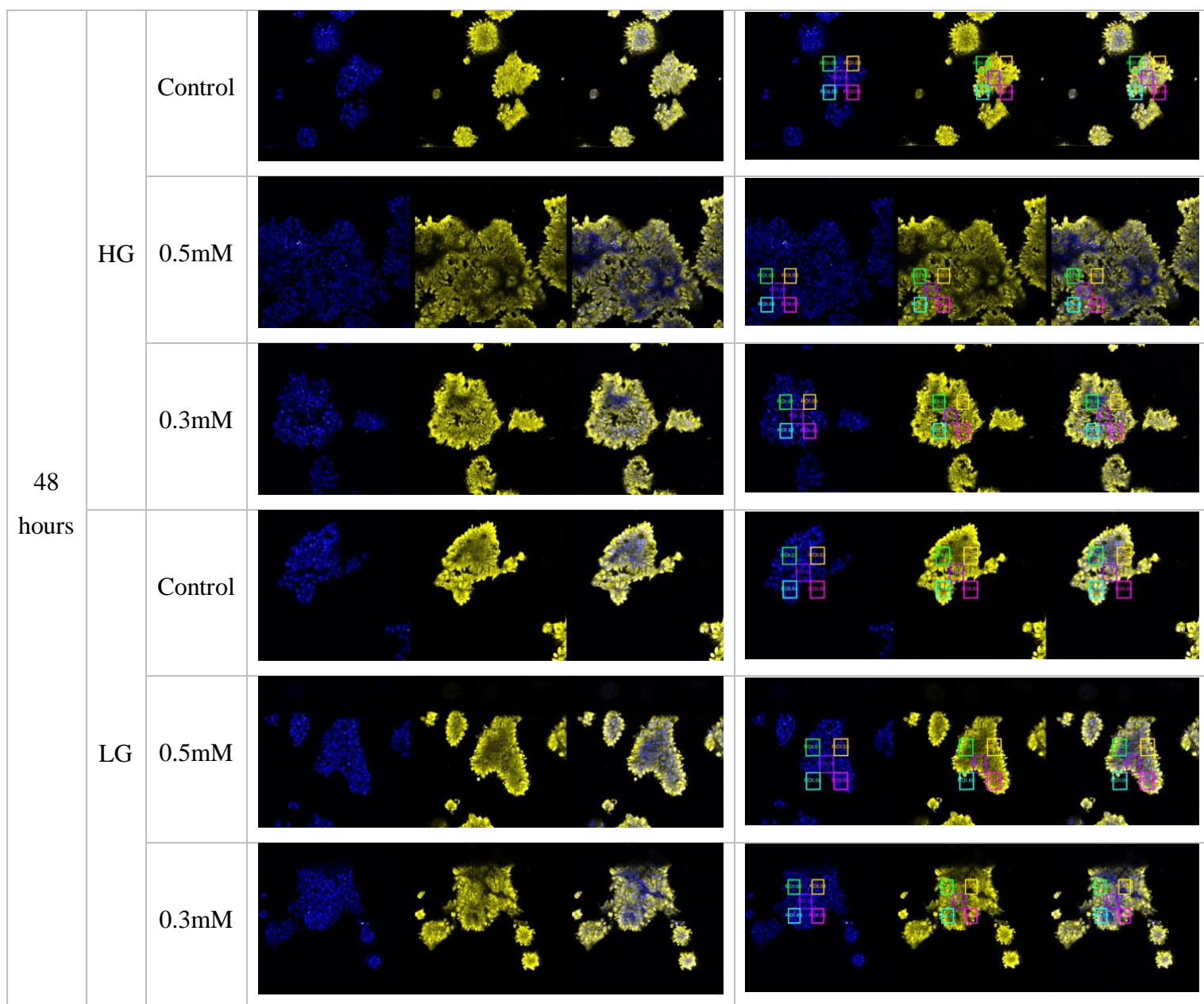
		0.5mM		
		0.3mM	NO IMAGES WERE AVAILABLE	

Table 5 Images taken on the Leica Confocal Microscope after analysis using Leica Application Suite 2.0 to add regions of interest to collect data of OCT1 in yellow using antibody SLC22A compared to the nucleus in blue stained with hoeschst in colorectal cancer cell line SW948. The treatment conditions shown are 6 hours, 12 hours, 24 hours and 48 hours using high glucose labelled HG and low glucose labelled LG with metformin treatments of 0.5mM and 3.0mM including a control which was used to compare the changes in OCT1 using the regions of interest. The images were taken to determine the location of OCT1.

Treatment conditions			Without Region of Interest	Added Region of Interest
6 hours	HG	Control		
		0.5mM		
		0.3mM		



		0.3mM		
24 hours	HG	Control		
		0.5mM		
		0.3mM		
	LG	Control		
		0.5mM		
		0.3mM		



The images presented in tables 3 and 4 represent the locations on each sample image in which was used for quantification to compare the ratio of OCT1:Nucleus using the histogram tool on Leica LASX software.

4.4.2 Oct1 Expression Changes With An Increase In Concentration Of Metformin

Ratio of OCT1 in colorectal cancer cell line SW1116 compared to cell nucleus as a percentage against the control sample for each glucose concentration and time interval

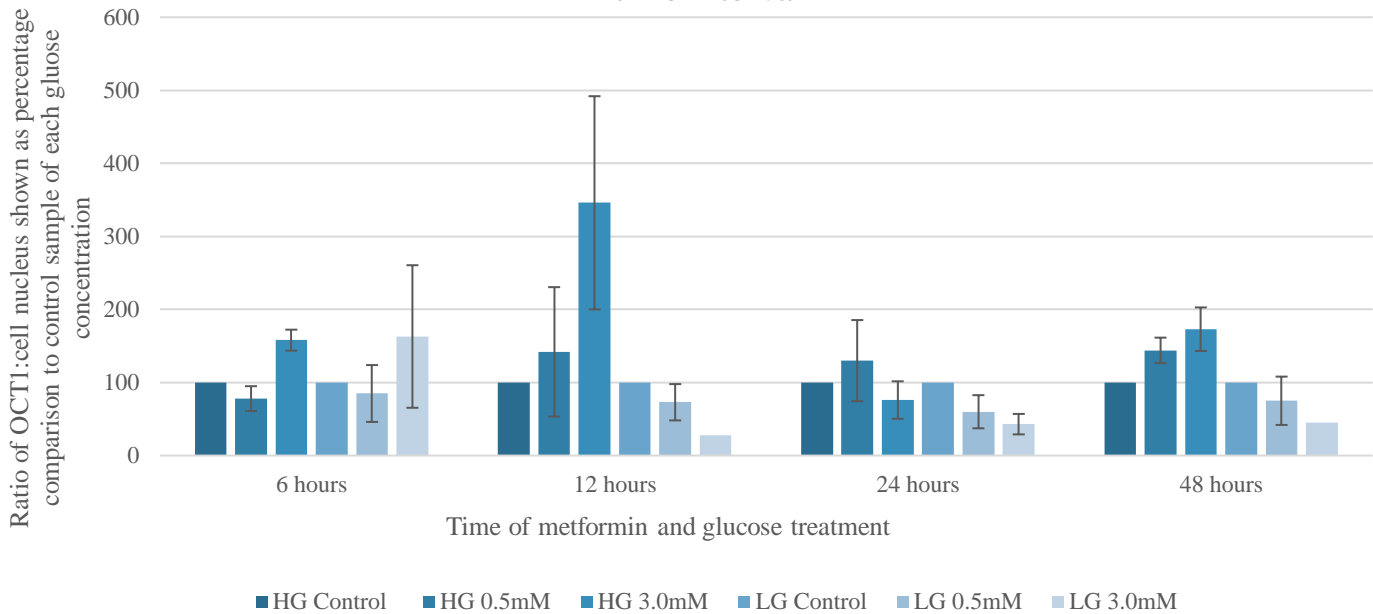


Figure 20 Ratio of OCT1 against cell nucleus using data from quantification on the Leica Application Suite using five regions of interest. The results are presented as a percentage compared to the control sample for concentrations of metformin (0.5mM, 3.0mM and a control) for high glucose (HG) and low glucose (LG) concentrations.

Using the five regions of interest shown in tables 3 and 4, the grey scale values for OCT1 and cell nucleus were used to create a ratio value for each condition. The averages for each ratio for high and low glucose, and metformin, were normalised against the control sample for each glucose concentration. All of the high glucose samples were normalised against the control for that concentration, and time period, to give a percentage comparison to the control to show if the ratio of OCT1:cell nucleus changed based on metformin concentration. In figure 20 above for SW1116, there is a fairly consistent reduction in OCT1 from the low glucose control when metformin is added, and this seems to be the case from 12-48 hours, although not at the 6 hours. In the high glucose samples there were a few inconsistencies in results although, changes do occur.

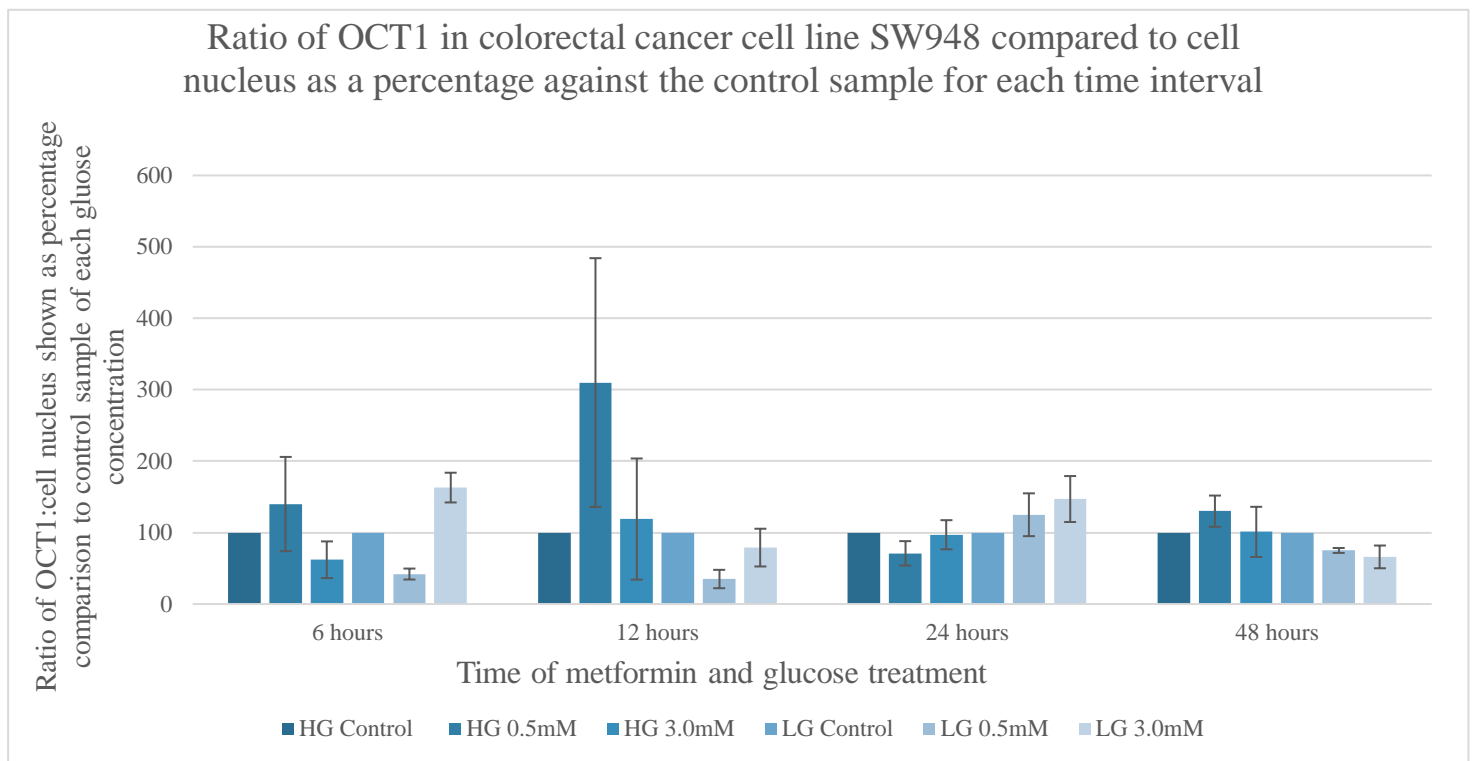


Figure 21 Ratio of OCT1 against cell nucleus using data from quantification on the Leica Application Suite using five regions of interest. The results are presented as a percentage compared to the control sample for concentrations of metformin (0.5mM, 3.0mM and a control) for high glucose (HG) and low glucose (LG) concentrations.

Analysis of SW948 in figure 21 shows that the high glucose samples appear to have an increase in OCT1 expression in high glucose when the metformin concentration is 0.5mM, but then decreases with 3.0mM, at 6, 12, and 48 hour samples. The 24 hour samples for low glucose are also giving different results to the 6, 12, and 48 as they indicate that in low glucose the presence of OCT1 drops when 0.5mM of metformin is compared to the control, with all being almost 50% of the control. The data used to create figures 20 and 21 are in the appendix.

5 Discussion

5.1 Glucose Concentrations Effect The Growth of Colorectal Cancer Cells

Initial observations during culturing and performing the first growth assays to assess the doubling times gave early indication that the high glucose and physiological low glucose concentrations had different effects on the two cancer cells lines. First, from looking at the 6 well plates during growth, the high glucose samples media had turned a very yellow colour, this indicates active metabolism and causes the pH of the media to drop due to the acidity²⁹. This was occurring much quicker with SW948 than SW1116 suggesting that they would take up the glucose and metabolise at a quick rate.

Glucose also had an effect during cell growth assay to determine doubling time, in both SW948 and SW1116 there were difference in cell growth between the glucose concentrations, and SW1116 especially appeared to grow better in low glucose initially, this could be because SW1116 take longer to attach to the flask surface, and also take a longer time to detach with trypsin, and this often leads to many cells people lost in the process. In addition, SW1116 may appear to grow better in physiological low glucose when really they don't crave the higher concentrations of glucose to survive and favour OXPHOS this could indicate why they also grow slower than SW948. Cells grown in lower concentrations of glucose depend on OXPHOS, and as SW1116 favour this already, this could suggest the quicker growth³⁰. SW948 on the other hand, thrive in the glucose rich environment, some cell lines become much more aggressive with their growth when glucose concentrations are increased, causing increased growth and migration³¹. T tests were performed to compare high and low glucose in both cells lines and was calculated that there is a significant difference between glucose concentrations, and was true for both cells lines.

5.2 SW948 Are More Glycolytic Compared To The OXPHOS Reliant SW1116

As discussed above, SW948 are glycolytic cells and grow well in high glucose conditions, whereas SW1116 are dependant more on the mitochondrial pathways to produce ATP for growth. There are significant differences between cell lines SW948 and SW1116, both MST and GST graphs categorised SW948 to be more energetic and glycolytic opposed to SW1116 aerobic and often less energetic behaviours (Fig10-13). Cancer cells are often expected to switch to a more glycolytic profile to avoid death during hypoxia³², and SW1116 could struggle to shift, the MTS for SW1116 did adopt a more glycolytic profile when exposed to 3.0mM of metformin compared to a control sample with no metformin (Fig13).

The profile of SW948 without metformin, with high glucose conditions had a highly energetic profile on the MTS (Fig10), this assay was performed with glucose in the media throughout so would have been actively using the glucose during the assay, the cells were less active in the low glucose conditions. As SW948 are more glycolytic, they will be more suited to switching to using glycolysis when the mitochondria is damaged due to stress on the cell. Metformin inhibit the ability for the mitochondria to produce energy causing an increase in glycolysis, if the cell isn't sufficiently adapt to switch, then growth decreases ³³. SW948 are more proficient during these conditions.

5.3 Alamar Blue And Brdu Show That Increases In Glucose Concentrations Increase The Effects Of Metformin

Alamar Blue viability assay and BrdU proliferation assays directed the course of experiments to be performed using 0.5mM and 3.0mM of metformin. Both concentrations were selected as they were not only suitable concentrations to relate research to a more realistic working environment but they also presented comparable results. Both assays, had distinct changes in cell results when 0.5mM of metformin was compared to a control with no metformin, therefore suggesting that there is effects on the cell growth at 0.5mM, and have been shown to have effects at 0.6mM³³. 3.0mM of metformin is suitable to use as higher concentrations

would not typically be expected to be useful when relating experiments to what could be relevant in a human body³⁴. The amount of metformin introduced into both assays were directly linked to decrease in cell growth when comparing to a control with no metformin, and even more effective in the higher glucose concentration compared to the physiological low glucose. Studies performed in the liver, have found that metformin inhibits the effect of glucose³⁵, the same study suggest that 5mM of metformin is required to obtain any compelling inhibition in complex 1 activity, again in the liver. Complex 1 on the ETC is where metformin is transported by OCT1, so if metformin is required in high concentrations to have an effect on complex 1, then this will also be linked to expression of OCT1. To contradict that discovery, it was found that in vivo as little as 0.45mM metformin caused 50% inhibition in peripheral blood mononuclear cells³⁶. Expected metformin and glucose concentrations used for trials differ between area being studies and although trials have not thus far been successful, the processed of metformin on colorectal cancer differ from that of studies in which have tried higher concentrations of metformin^{37,38}.

5.4 OCT1 Is Related To The Performance Of Metformin On Colorectal Cancer Cells

OCT1, the transporter for metformin into the cell was imaged using the confocal microscope and is located on the outside of the cell (Fig 18). The full mechanisms of OCT1 are still yet to be discovered and most research thus far largely involved the liver but do link OCT1 to the uptake of metformin and been suggested that colorectal cancer to be the most successful in enabling metformin to perform^{9,39}. The images of SW948 and SW1116 (tables 3&4) analysed by LASX were all consistent as to the staining of OCT1 (gene *SLC22A1*) showed in yellow were around the nucleus of the cell, shown in blue. Images in which were taken with large areas of cells together, had very little OCT1 staining in the circle of cells which had formed together. This could either be that the cells were in such a large number that one of the antibodies could not penetrate the centre to stain the cells in the middle or, that when the cell are clumped together and metformin is introduced, it fails to reach the cells in the middle, almost as the cells on the outside took up the majority of the metformin, therefore being

stained more intensity than the centre, due to the larger amount of OCT1 to transport the metformin.

To assess is metformin concentration effect OCT1 gene expression, quantification of the images in tables 3 and 4 were performed using Leica LASX. Five ROI's were used to assess the ratio of OCT1:Hoeschst to see what scales OCT1 were present. Protocol was in place for selecting the cells for the imaging and ratios calculated. SW1116 had consistence changes to amount of OCT1, in that it decreased as metformin increased in 75% of the conditions. SW948 followed similar changes after 48 hours of treatment, but didn't change considerably after 6, 12 or 24 hours. This indicates that with an increase of metformin the expression of OCT1 decreased, this can be a defence mechanism of the cell to stop metformin from being transported.

6 Considerations For Further Research And Closing Conclusions

6.1 Continuation of Research

More specific research is being performed to look at many variables of how the future of metformin treatment can be adapted and how to best suit treatment for individuals. Looking at personalised medicine and how individuals may gain from metformin treatment for colorectal cancer, studies include information about prescription medicine in which people take which could affect how metformin is received. It found that some drugs such as depression drugs or proton pump inhibitors change the mechanisms of metformin⁴⁰.

OCT1 to be analysed using flow cytometry, to find more information about how metformin changes expression of OCT1, although many studies discuss how there is little change in the liver, they state that the processes in the colon are different^{40,41}. The contrasting behaviours between cell lines, glucose concentrations and metformin concentrations shows the importance of determining how each variable changes the expression of OCT1 and the effects of metformin. The media used to culture the cells also changes growth behaviours of cells, and the extra supplements added change the profile of each cell line and will exhibit different profiles^{16,42}.

6.2 Conclusions

While the understanding about the processes of colorectal cancer cells expands, they continuously change depending on environment, and as we further develop our technology to improve our ability to perform more sensitive and evasive techniques, the closer to being able to create a treatment model is achieved. This research has shown that colorectal cancer cells changed their profile to continue to flourish even in stressed environments, and many variables such as glucose concentration, cell line and metformin concentrations create a barrier from achieving a 'one fits all' solution to the effects of colorectal cancer. OCT1 certainly plays a role in the uptake of metformin, which together is closely linked to the way the cells proliferate and continue to thrive⁴³, displaying the brutal resilience of such a fatal disease. Further research into more specific processes such as continuation into how the cancer cells shift profiles when stress is introduced may help develop processes to inhibit this change.

7 References

1. Jang M, Kim SS, Lee J. Cancer cell metabolism: Implications for therapeutic targets. *Exp Mol Med*. 2013;45(10):e45-8. doi:10.1038/emm.2013.85.
2. Suganuma K, Miwa H, Imai N, et al. Energy metabolism of leukemia cells: glycolysis versus oxidative phosphorylation. *Leuk Lymphoma*. 2010;51(11):2112-2119. doi:10.3109/10428194.2010.512966.
3. Martínez-Reyes I, Diebold LP, Kong H, et al. TCA Cycle and Mitochondrial Membrane Potential Are Necessary for Diverse Biological Functions. *Mol Cell*. 2016;61(2):199-209. doi:10.1016/j.molcel.2015.12.002.
4. Fang S, Fang X. Advances in glucose metabolism research in colorectal cancer. *Biomed reports*. 2016;5(3):289-295. doi:10.3892/br.2016.719.
5. Baysal BE1, Ferrell RE, Willett-Brozick JE, Lawrence EC, Myssiorek D, Bosch A, van der Mey A, Taschner PE, Rubinstein WS, Myers EN, Richard CW 3rd, Cornelisse CJ, Devilee P DB. Mutations in SDHD, a mitochondrial complex II gene, in hereditary paraganglioma. *Science (80-)*. 2000;204(February):1998-2001.
6. Hanahan D, Weinberg RA. Hallmarks of cancer: The next generation. *Cell*. 2011;144(5):646-674. doi:10.1016/j.cell.2011.02.013.
7. Winawer S, Fletcher R, Rex D, et al. Colorectal cancer screening and surveillance: Clinical guidelines and rationale - Update based on new evidence. *Gastroenterology*. 2003;124(2):544-560. doi:10.1053/gast.2003.50044.
8. Kuipers EJ, Grady WM, Lieberman D, et al. Colorectal cancer. *Nat Rev Dis Prim*. 2015;1. doi:10.1038/nrdp.2015.65.
9. Florez JC. The pharmacogenetics of metformin. *Diabetologia*. 2017;60(9):1648-1655. doi:10.1007/s00125-017-4335-y.
10. Madiraju AK, Erion DM, Rahimi Y, et al. Metformin suppresses gluconeogenesis by

- inhibiting mitochondrial glycerophosphate dehydrogenase. *Nature*. 2014;510(7506):542-546. doi:10.1038/nature13270.Metformin.
11. Kim JH, Lee KJ, Seo Y, et al. Effects of metformin on colorectal cancer stem cells depend on alterations in glutamine metabolism. *Sci Rep*. 2018;8(1):409. doi:10.1038/s41598-017-18762-4.
 12. El-Mir M-Y, Nogueira V, Fontaine E, Avéret N, Rigoulet M, Leverve X. Dimethylbiguanide Inhibits Cell Respiration via an Indirect Effect Targeted on the Respiratory Chain Complex I Dimethylbiguanide Inhibits Cell Respiration via an Indirect Effect Targeted on the Respiratory Chain Complex I *. *J Biol Chem*. 2000;275(1):223-228. doi:10.1074/jbc.275.1.223.
 13. Luengo A, Sullivan LB, Heiden VGV. Understanding the complex-I-ty of metformin action: Limiting mitochondrial respiration to improve cancer therapy. *BMC Biol*. 2014;12(1):1-4. doi:10.1186/s12915-014-0082-4.
 14. Gui DY, Sullivan LB, Luengo A, et al. Environment Dictates Dependence on Mitochondrial Complex I for NAD⁺ and Aspartate Production and Determines Cancer Cell Sensitivity to Metformin. *Cell Metab*. 2016;24(5):716-727. doi:10.1016/j.cmet.2016.09.006.
 15. Heckman-Stoddard BM, DeCensi A, Sahasrabudhe V V., Ford LG. Repurposing metformin for the prevention of cancer and cancer recurrence. *Diabetologia*. 2017;60(9):1639-1647. doi:10.1007/s00125-017-4372-6.
 16. Tannock IF, Kopelyan I. Influence of glucose concentration on growth and formation of necrosis in spheroids derived from a human bladder cancer cell line. *Cancer Res*. 1986;46(6):3105-3110.
 17. Ishida T, Shimamoto T, Ozaki N, et al. Investigation of the influence of glucose concentration on cancer cells by using a microfluidic gradient generator without the induction of large shear stress. *Micromachines*. 2016;7(9). doi:10.3390/mi7090155.
 18. Strimbu K, Tavel J a. What are Biomarkers? *Curr Opin HIV AIDS*. 2011;5(6):463-466.

doi:10.1097/COH.0b013e32833ed177.What.

19. Ludwig JA, Weinstein JN. Biomarkers in cancer staging, prognosis and treatment selection. *Nat Rev Cancer*. 2005;5(11):845-856. doi:10.1038/nrc1739.
20. Shu Y, Sheardown S a S, Brown C, et al. Effect of genetic variation in the organic cation transporter 1 (OCT1) on metformin action. *J Clin* 2007;117(5):1422-1431. doi:10.1172/JCI30558DS1.
21. Chen L, Shu Y, Liang X, et al. OCT1 is a high-capacity thiamine transporter that regulates hepatic steatosis and is a target of metformin. *Proc Natl Acad Sci*. 2014;111(27):9983-9988. doi:10.1073/pnas.1314939111.
22. Jonker JW, Wagenaar E, Mol CAAM, et al. Reduced Hepatic Uptake and Intestinal Excretion of Organic Cations in Mice with a Targeted Disruption of the Organic Cation Transporter 1 (Oct1 [Slc22a1]) Gene. *Mol Cell Biol*. 2001;21(16):5471-5477. doi:10.1128/MCB.21.16.5471.
23. Lines OC, Hilgendorf C, Ahlin G, et al. Expression of Thirty-six Drug Transporter Genes in Human. *Basic Clin Pharmacol Toxicol*. 2007;35(8):1333-1340. doi:10.1124/dmd.107.014902.ularly.
24. Hargreaves AJ, Sachana M, Flaskos J. *Cell Culture Techniques*. Vol 56.; 2011. doi:10.1007/978-1-61779-077-5.
25. Millipore. Muse™ Count & Viability Kit.
26. Agilent. 5. Loading the Agilent Seahorse XFe 96 Sensor Cartridge Injection Ports. (2):4-7. http://www.agilent.com/cs/library/usermanuals/public/DAY_OF_LOADING_CARTRIDGE_XFe96-XF96.pdf.
27. Wojtowicz JM, Kee N. BrdU assay for neurogenesis in rodents. *Nat Protoc*. 2006;1(3):1399-1405. doi:10.1038/nprot.2006.224.
28. Erikstein BS, Hagland HR, Nikolaisen J, et al. Cellular stress induced by resazurin leads to autophagy and cell death via production of reactive oxygen species and

- mitochondrial impairment. *J Cell Biochem.* 2010;111(3):574-584.
doi:10.1002/jcb.22741.
29. Phelan K, May KM. Basic techniques in mammalian cell tissue culture. *Curr Protoc Cell Biol.* 2015;2015(March):1.1.1-1.1.22. doi:10.1002/0471143030.cb0101s66.
 30. Jose C, Bellance N, Rossignol R. Choosing between glycolysis and oxidative phosphorylation: A tumor's dilemma? *Biochim Biophys Acta - Bioenerg.* 2011;1807(6):552-561. doi:10.1016/j.bbabi.2010.10.012.
 31. Hou Y. High glucose levels promote the proliferation of breast cancer cells through GTPases. 2017:429-436.
 32. Vander Heiden M, Cantley L, Thompson C. Understanding the Warburg effect: The metabolic Requirements of cell proliferation. *Science (80-).* 2009;324(5930):1029-1033. doi:10.1126/science.1160809.Understanding.
 33. Mogavero A, Maiorana MV, Zanutto S, et al. Metformin transiently inhibits colorectal cancer cell proliferation as a result of either AMPK activation or increased ROS production. *Sci Rep.* 2017;7(1):1-12. doi:10.1038/s41598-017-16149-z.
 34. Kajbaf F, De Broe ME, Lalau JD. Therapeutic Concentrations of Metformin: A Systematic Review. *Clin Pharmacokinet.* 2016;55(4):439-459. doi:10.1007/s40262-015-0323-x.
 35. He L, Wondisford FE. Metformin action: Concentrations matter. *Cell Metab.* 2015;21(2):159-162. doi:10.1016/j.cmet.2015.01.003.
 36. Piel S, Ehinger JK, Elmér E, Hansson MJ. Metformin induces lactate production in peripheral blood mononuclear cells and platelets through specific mitochondrial complex I inhibition. *Acta Physiol.* 2015;213(1):171-180. doi:10.1111/apha.12311.
 37. Lyssiotis CA, Kimmelman AC. Metabolic Interactions in the Tumor Microenvironment. *Trends Cell Biol.* 2017;xx:1-13. doi:10.1016/j.tcb.2017.06.003.
 38. Miyo M, Konno M, Nishida N, et al. Metabolic Adaptation to Nutritional Stress in

- Human Colorectal Cancer. *Sci Rep*. 2016;6(December):38415. doi:10.1038/srep38415.
39. Wang Y peng, Song G he, Chen J, et al. Elevated OCT1 participates in colon tumorigenesis and independently predicts poor prognoses of colorectal cancer patients. *Tumor Biol*. 2016;37(3):3247-3255. doi:10.1007/s13277-015-4080-0.
 40. Dujic T, Zhou K, Donnelly LA, Tavendale R, Palmer CN, Pearson ER. Association of Organic Cation Transporter 1 with Intolerance to Metformin in Type 2 Diabetes: A GoDARTS Study. *Diabetes*. 2014;64(5):1786-1793. doi:10.2337/db14-1388.
 41. Yang G, Sau C, Lai W, Cichon J, Li W. The Oct1 transcription factor and epithelial malignancies: Old protein learns new tricks. 2015;344(6188):1173-1178. doi:10.1126/science.1249098.Sleep.
 42. Thangaraju M, Carswell KN, Prasad PD, Ganapathy V. Colon cancer cells maintain low levels of pyruvate to avoid cell death caused by inhibition of HDAC1/HDAC3. *Biochem J*. 2009;417(1):379-389. doi:10.1042/BJ20081132.
 43. Dujic T, Zhou K, Yee SW, et al. Variants in Pharmacokinetic Transporters and Glycemic Response to Metformin: A Metgen Meta-Analysis. *Clin Pharmacol Ther*. 2017;101(6):763-772. doi:10.1002/cpt.567.

Appendix

Cell Proliferation of SW948 and SW1116 in High and Low glucose

Appendix Table 1 Cell Count for SW948 and SW1116 in high and low glucose used for doubling time

	24 hours			
<u>SW948</u>				
	Run 1	Run 2	Run 3	Averages
High glucose 25Mm A	116000	119000	123000	119333
High glucose 25Mm B	105000	110000	107000	107333
High glucose 25Mm C	136000	135000	132000	134333
Low glucose 5mM A	136000	137000	136500	136500
Low glucose 5Mm B	97700	94000	96800	96167
Low glucose 5Mm C	98900	108000	111000	105967
	48 hours			
	Cell count	Cell count	Cell count	Averages
High glucose 25Mm A	353000	362000	351000	355333
High glucose 25Mm B	350000	348000	371000	356333
High glucose 25Mm C	310000	328000	301000	313000
Low glucose 5mM A	318000	321000	343000	327333
Low glucose 5Mm B	397000	433000	428000	419333
Low glucose 5Mm C	425000	457000	436000	439333
	72 hours			
	Cell count	Cell count	Cell count	Averages
High glucose 25Mm A	576000	591000	587000	584667
High glucose 25Mm B	535000	583000	648000	588667
High glucose 25Mm C	543000	513000	533000	529667
Low glucose 5mM A	705000	777000	788000	756667
Low glucose 5Mm B	741000	709000	759000	736333
Low glucose 5Mm C	599000	590000	618000	602333

	24 hours			
<u>SW1116</u>				
	Run 1	Run 2	Run 3	Averages
High glucose 25Mm A	236000	259000	239000	244667
High glucose 25Mm B	229000	233000	232000	231333
High glucose 25Mm C	332000	334000	341000	335667
Low glucose 5mM A	683000	620000	591000	631333
Low glucose 5Mm B	263000	304000	276000	281000
Low glucose 5Mm C	331000	337000	308000	325333
	48 hours			
	Cell count	Cell count	Cell count	Averages
High glucose 25Mm A	283000	286000	298000	289000
High glucose 25Mm B	251000	268000	272000	263667
High glucose 25Mm C	212000	206000	221000	213000
Low glucose 5mM A	755000	584000	627000	655333
Low glucose 5Mm B	595000	590000	587000	590667
Low glucose 5Mm C	483000	404000	418000	435000
	72 hours			
	Cell count	Cell count	Cell count	Averages
High glucose 25Mm A	284000	279000	301000	288000
High glucose 25Mm B	577000	526000	492000	531667
High glucose 25Mm C	578000	417000	509000	501333
Low glucose 5mM A	492000	505000	510000	502333
Low glucose 5Mm B	665000	601000	436000	567333
Low glucose 5Mm C	563000	535000	522000	540000

Metformin concentration (mM)	SW1116 Low Glucose fluorescence 48 hours	SW1116 High Glucose fluorescence 48 hours
Control	77693151.5	50422672.8
0.5	64607966.4	49532132.8
1	57846417.6	45837103.5
3	60945424.8	48605028.8
5	55693624.8	43731072.8
10	55380206.4	39383632.8

Alamar Blue Fluorescence Used for Results. Negative and Backgrounds Removed and Results

Appendix Table 2 SW1116 Alamar Blue fluorescence of 48 hours of treatment. Not normalised to the control

Appendix Table 3 Appendix Table 2 SW948 Alamar Blue fluorescence of 48 hours of treatment. Not normalised to the

Metformin concentrations (mM)	SW948 Low Glucose fluorescence 48 hours	SW948 High Glucose fluorescence 48 hours
Control	29460441.5	26207417.0
0.5	23943226.7	21124422.7
1	24779836.7	23039104.5
3	22980686.7	22620161.5
5	21845001.0	16616989.5
10	20501193.3	16300806.3

control

BrdU Proliferation Assay Absorbance Value for SW948 and SW1116 after 40 hours

Averages of 3 replicates	SW1116	
	Low Glucose 1g/L	High Glucose 4.5g/L
Control 0mM	100	100
0.5mM	78.20676657	93.63791998
1.0mM	79.03280915	60.93472267
3.0mM	51.39081501	52.94604028
5.0mM	49.76994429	60.52011808
Averages of 3 replicates	SW948	
	Low Glucose 1g/L	High Glucose 4.5g/L
Control 0mM	100	100
0.5mM	123.6845325	93.59543176
1.0mM	110.0762179	51.55705149
3.0mM	108.1609599	60.29010146
5.0mM	94.88589572	64.07603615

Appendix Table 4 BrdU assay for SW948 and SW1116 after 48hours with average values normalised against the control to give % change.

Confocal imaging OCT1:Nucleus grey scale values using five regions of interest

SW1116 6 hours

HG Control						
	ROI 1	ROI 2	ROI 3	ROI 4	ROI 5	Average
Hoechst grey scale	10.32	7.21	8.79	7.52	14.25	9.618
OCT1 grey scale	8.98	5.94	13.12	10.14	12.67	10.17
Ratio	0.870155039	0.82385576	1.49260523	1.34840426	0.88912281	<u>1.08482862</u>
	ROI Area	1,468ul	12.49 pixels			
HG 0.5mM						
	ROI 1	ROI 2	ROI 3	ROI 4	ROI 5	Average
Hoechst grey scale	6.66	16.2	18.99	7.88	14.74	12.894
OCT1 grey scale	5.17	11.18	13.46	8.65	14.8	10.652
Ratio	0.776276276	0.69012346	0.7087941	1.09771574	1.00407056	<u>0.85539603</u>
	ROI Area	1,468ul	6.23 pixels			
HG 3.0mM						
	ROI 1	ROI 2	ROI 3	ROI 4	ROI 5	Average
Hoechst grey scale		13.65	11.41		12.63	12.5633333
OCT1 grey scale		23.1	21.5		19.91	21.5033333
Ratio		1.69230769	1.88431201		1.57640538	<u>1.71767503</u>
	ROI Area	1,468				
LG Control						
	ROI 1	ROI 2	ROI 3	ROI 4	ROI 5	Average
Hoechst grey scale	15.52	11.17	11.88			12.8566667
OCT1 grey scale	13.49	12.38	13.2			13.0233333
Ratio	0.869201031	1.10832587	1.11111111			<u>1.029546</u>
	ROI Area	1,468ul	16.18 pixels			
LG 0.5mM						
	ROI 1	ROI 2	ROI 3	ROI 4	ROI 5	Average
Hoechst grey scale	3.29	12.21	5.8	11.47		8.1925
OCT1 grey scale	3.28	6.13	8.05	7.13		6.1475
Ratio	0.996960486	0.5020475	1.38793103	0.62162162		<u>0.87714016</u>
LG 3.0mM						

	ROI 1	ROI 2	ROI 3	ROI 4	ROI 5	Average
Hoechst grey scale	6.43	4.88	7.17	6.29	4.13	5.78
OCT1 grey scale	17.79	6.64	5.89	10.02	7.71	9.61
Ratio	2.766718507	1.36065574	0.82147838	1.59300477	1.86682809	<u>1.6817371</u>
	ROI area	1,468ul	28.78 pixels			

SW1116 12 hours

HG Control							
	ROI 1	ROI 2	ROI 3	ROI 4	ROI 5	Average	
Hoechst grey scale	14.95	17.87	19	15.81	30.14	19.554	
OCT1 grey scale	20.75	34.81	14.02	9.88	38.89	23.67	
Ratio	1.38795987	1.94795747	0.737894737	0.62492094	1.29031188	<u>1.19780898</u>	
	ROI Area	1,468ul	10.28 pixels				
HG 0.5mM							
	ROI 1	ROI 2	ROI 3	ROI 4	ROI 5	Average	
Hoechst grey scale	6.7	17.29	15.94	11.8	25.14	15.374	
OCT1 grey scale	15.22	8.17	12.23	19.4	9.48	12.9	
Ratio	2.27164179	0.47252747	0.767252196	1.6440678	0.37708831	<u>1.10651551</u>	
	ROI Area	1,468ul	15.63 kpixels				
HG 3.0mM							
	ROI 1	ROI 2	ROI 3	ROI 4	ROI 5	Average	
Hoechst grey scale	2.78	4.59	4.59	3.43	3.98	3.874	
OCT1 grey scale	11.02	14.79	17.92	24.36	10.16	15.65	
Ratio	3.96402878	3.22222222	3.904139434	7.10204082	2.55276382	4.14903901	
					One cell	<u>0.53</u>	
LG Control							
	ROI 1	ROI 2	ROI 3	ROI 4	ROI 5	Average	
Hoechst grey scale	7.850	5.720	6.840			6.803	
OCT1 grey scale	9.390	12.500	17.420			13.103	
Ratio	1.19617834	2.18531469	2.546783626			<u>1.976</u>	
LG 0.5mM							

	ROI 1	ROI 2	ROI 3	ROI 4	ROI 5	Average
Hoechst grey scale	15.220	12.060	13.090			13.457
OCT1 grey scale	14.990	23.700	18.560			19.083
Ratio	0.9848883	1.96517413	1.417876241			<u>1.456</u>
LG 3.0mM						
	ROI 1	ROI 2	ROI 3	ROI 4	ROI 5	Average
Hoechst grey scale	12.260	12.610	8.790		8.370	10.508
OCT1 grey scale	6.830	7.190	5.170		4.750	5.985
Ratio	0.55709625	0.57018239	0.588168373			<u>0.572</u>

SW1116 24 hours

	ROI 1	ROI 2	ROI 3	ROI 4	ROI 5	Average
HG Control						
Hoechst grey scale	24.56	17.15	19.13	22.18	11.49	18.902
OCT1 grey scale	20.45	16.05	13.96	13.3	9.37	14.626
Ratio	0.83265472	0.93586006	0.72974386	0.59963931	0.81549173	0.78267794
HG 0.5mM						
	ROI 1	ROI 2	ROI 3	ROI 4	ROI 5	Average
Hoechst grey scale	16.3	12.96	16.31	16.35	17.93	15.97
OCT1 grey scale	21.07	21.29	10.64	10.64	15.85	15.898
Ratio	1.29263804	1.64274691	0.65236052	0.65076453	0.88399331	1.02450066
HG 3.0mM						
	ROI 1	ROI 2	ROI 3	ROI 4	ROI 5	Average
Hoechst grey scale	16.13	17.52	16.14			16.5966667
OCT1 grey scale	8.62	14.42	7.05			10.03
Ratio	0.53440794	0.82305936	0.43680297			0.59809009
LG Control						
	ROI 1	ROI 2	ROI 3	ROI 4	ROI 5	Average
Hoechst grey scale	7.02	15.7	18.9			13.8733333
OCT1 grey scale	21.29	48.07	38.24			35.8666667

Ratio	3.03276353	3.06178344	2.02328042			2.70594247
LG 0.5mM						
	ROI 1	ROI 2	ROI 3	ROI 4	ROI 5	Average
Hoechst grey scale	9.48	18.32	14.42	1.34	8.95	10.502
OCT1 grey scale	18.43	18.11	16.86	3.37	14.62	14.278
Ratio	1.94409283	0.98853712	1.16920943	2.51492537	1.63351955	1.65005686
LG 3.0mM						
	ROI 1	ROI 2	ROI 3	ROI 4	ROI 5	Average
Hoechst grey scale	11.12	12.06	22.56	16.66	16.36	15.752
OCT1 grey scale	14.18	18.54	12.19	21.14	21.59	17.528
Ratio	1.27517986	1.53731343	0.54033688	1.26890756	1.31968215	1.18828398

SW1116 48 hours

HG Control						
	ROI 1	ROI 2	ROI 3	ROI 4	ROI 5	Average
Hoechst grey scale	11.85	10.03	15.02	6.32	10.22	10.688
OCT1 grey scale	19.38	19.09	16.74	9.64	19.77	16.924
Ratio	1.63544304	1.90329013	1.11451398	1.52531646	1.93444227	1.62260117
HG 0.5mM						
	ROI 1	ROI 2	ROI 3	ROI 4	ROI 5	Average
Hoechst grey scale	11.13	15.23	13.34			13.2333333
OCT1 grey scale	29.67	32.87	29.3			30.6133333
Ratio	2.66576819	2.15824032	2.1964018			2.34013677
HG 3.0mM						
	ROI 1	ROI 2	ROI 3	ROI 4	ROI 5	Average
Hoechst grey scale	8.53	11.95	7.12	11.57	13.07	10.448
OCT1 grey scale	22.3	41.36	15.24	34	37.92	30.164
Ratio	2.61430246	3.46108787	2.14044944	2.9386344	2.90130069	2.81115497
LG Control						
	ROI 1	ROI 2	ROI 3	ROI 4	ROI 5	Average

	Hoechst grey scale	6.29	8.23	8.1	7.21	8.3	7.626
	OCT1 grey scale	26.43	28.45	20.75	28.16	35.09	27.776
	Ratio	4.20190779	3.45686513	2.5617284	3.90568655	4.22771084	3.67077974
	LG 0.5mM						
		ROI 1	ROI 2	ROI 3	ROI 4	ROI 5	Average
	Hoechst grey scale	9	12.72	13.06	7.49	10.22	10.498
	OCT1 grey scale	33.89	38.39	13.66	38.52	34.84	31.86
	Ratio	3.76555556	3.01808176	1.04594181	5.14285714	3.40900196	3.27628764
	LG 3.0mM						
		ROI 1	ROI 2	ROI 3	ROI 4	ROI 5	Average
	Hoechst grey scale	20.2					20.2
	OCT1 grey scale	33.99					33.99
	Ratio	1.68267327					1.68267327

SW948 6 hours

HG Control						
	ROI 1	ROI 2	ROI 3	ROI 4	ROI 5	Average
Hoechst grey scale	7.54	14.13	7.33	4.91	6.54	8.09
OCT1 grey scale	22.59	7.44	18.41	26.99	27.9	20.666
Ratio	2.99602122	0.52653928	2.51159618	5.49694501	4.26605505	3.15943135
	ROI Area	2,418.22 u2	8.10 pixels			
HG 0.5mM						
	ROI 1	ROI 2	ROI 3	ROI 4	ROI 5	Average
Hoechst grey scale	2.99	15.62	6.86	5.37	2.54	6.676
OCT1 grey scale	19.75	22.56	23.13	25.87	15.23	21.308
Ratio	6.60535117	1.44430218	3.37172012	4.81750466	5.99606299	4.44698822
	ROI Area					
HG 3.0mM						
	ROI 1	ROI 2	ROI 3	ROI 4	ROI 5	Average
Hoechst grey scale	5.89	8.7	6.72	5.56	5.48	6.47
OCT1 grey scale	15.23	6.38	13.86	15.49	9.56	12.104
Ratio	2.58573854	0.73333333	2.0625	2.78597122	1.74452555	1.98241373
	ROI Area	2,418.22 u2	8.10 pixels			
LG Control						
	ROI 1	ROI 2	ROI 3	ROI 4	ROI 5	Average
Hoechst grey scale	6.82	4.03	7.17	4.93	4.56	5.502
OCT1 grey scale	9.5	9.83	12.36	16.14	14.21	12.408
Ratio	1.39296188	2.43920596	1.72384937	3.27383367	3.11622807	2.38921579
	ROI Area	2,418.22 u2	8.10 pixels			
LG 0.5mM						
	ROI 1	ROI 2	ROI 3	ROI 4	ROI 5	Average
Hoechst grey scale	29.9	18.09	17.51	9.18	11.55	17.246
OCT1 grey scale	24.79	14.39	18.76	10.36	13.91	16.442
Ratio	0.82909699	0.79546711	1.07138778	1.12854031	1.204329	1.00576424
	ROI Area	2,418.22 u2	8.10 pixels			
LG 3.0mM						
	ROI 1	ROI 2	ROI 3	ROI 4	ROI 5	Average
Hoechst grey scale	5.75	8.94	5.72			6.80333333
OCT1 grey scale	19.43	35.05	25.01			26.4966667
Ratio	3.37913043	3.92058166	4.37237762	#DIV/0!	#DIV/0!	3.89465948
	ROI area	2,418.22 u2	8.10 pixels			

HG Control						
	ROI 1	ROI 2	ROI 3	ROI 4	ROI 5	Average
Hoechst grey scale	22.42	22.78	18.3	18.74	19.11	20.27
OCT1 grey scale	6.19	6.71	13.52	12.75	11.3	10.094
Ratio	0.27609277	0.29455663	0.73879781	0.68036286	0.59131345	0.51622471
	ROI Area	2,418.22 u2	8.10 pixels			
HG 0.5mM						
	ROI 1	ROI 2	ROI 3	ROI 4	ROI 5	Average
Hoechst grey scale	15.84	23.85	15.81	12.31	7.8	15.122
OCT1 grey scale	48.94	52	50.37	43.11	40.2	46.924
Ratio	3.08964646	2.1802935	3.18595825	3.50203087	5.15384615	3.42235505
	ROI Area	2,418.22 u2	8.10 pixels			
HG 3.0mM						
	ROI 1	ROI 2	ROI 3	ROI 4	ROI 5	Average
Hoechst grey scale	8.36	28.66	14.3	15.94	23.73	18.198
OCT1 grey scale	10.79	6.34	11.44	7.81	6.91	8.658
Ratio	1.29066986	0.22121424	0.8	0.48996236	0.29119258	0.61860781
	ROI Area	2,418.22 u2	8.10 pixels			
LG Control						
	ROI 1	ROI 2	ROI 3	ROI 4	ROI 5	Average
Hoechst grey scale	20.54	16.72	21.61	13.71	ROI 5	18.145
OCT1 grey scale	25.25	15.87	45.57	12.73		24.855
Ratio	1.22930867	0.94916268	2.10874595	0.92851933		1.30393416
	ROI Area	2,418.22 u2	8.10 pixels			
LG 0.5mM						
	ROI 1	ROI 2	ROI 3	ROI 4	ROI 5	Average
Hoechst grey scale	32.15	34.42	44.51	29.32	30.7	34.22

OCT1 grey scale	19.59	10.15	16.34	10.38	20.51	15.394
Ratio	0.60933126	0.29488669	0.36710851	0.35402456	0.66807818	0.45868584
	ROI Area	2,418.22 u2	8.10 pixels			
LG 3.0mM						
	ROI 1	ROI 2	ROI 3	ROI 4	ROI 5	Average
Hoechst grey scale	14.68	14.13	8.44			12.4166667
OCT1 grey scale	16.01	9.53	11.46			12.3333333
Ratio	1.09059946	0.67445152	1.35781991	#DIV/0!	#DIV/0!	1.04095696
	ROI Area	2,418.22 u2	8.10 pixels			

SW948 12 hours

SW948 24 hours

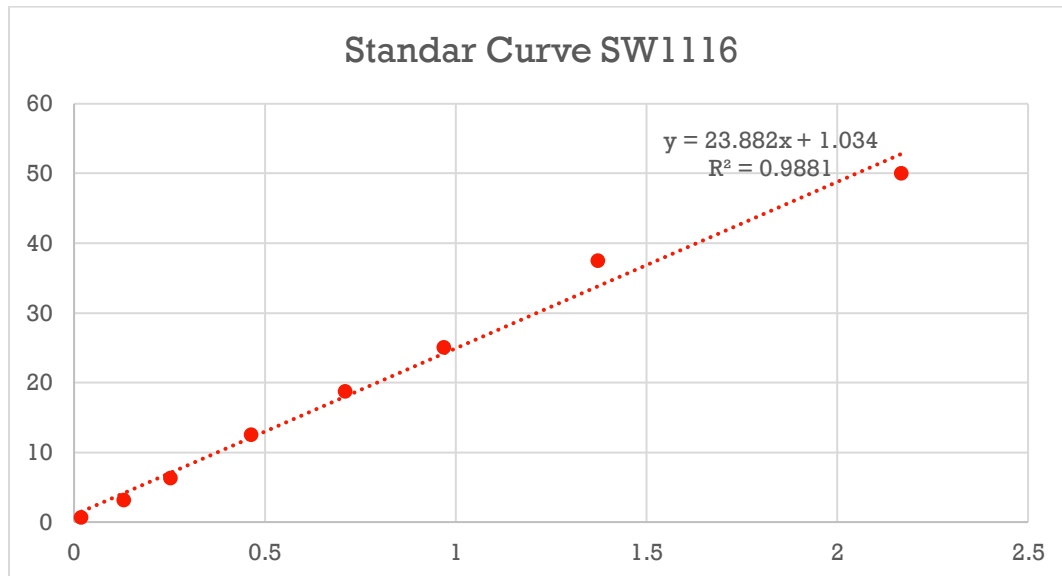
HG Control						
	ROI 1	ROI 2	ROI 3	ROI 4	ROI 5	Average
Hoechst grey scale	4.32	12.08	7.63		15.66	9.9225
OCT1 grey scale	5.84	17.24	7.21		22.43	13.18
Ratio	1.35185185	1.427152318	0.94495413		1.43231162	1.32829428
	ROI Area	2,418.22 u2	8.10 pixels			
HG 0.5mM						
	ROI 1	ROI 2	ROI 3	ROI 4	ROI 5	Average
Hoechst grey scale	13.7	24.1	13.76	17.01	12.26	16.166
OCT1 grey scale	15.55	13.98	14.61	15.04	13.24	14.484
Ratio	1.1350365	0.580082988	1.06177326	0.88418577	1.07993475	0.94820265
	ROI Area	2,418.22 u2	8.10 pixels			
HG 3.0mM						
	ROI 1	ROI 2	ROI 3	ROI 4	ROI 5	Average
Hoechst grey scale	18.39	16.65	18.63			17.89
OCT1 grey scale	18.03	24.62	26.35			23
Ratio	0.98042414	1.478678679	1.4143854			1.29116274
	ROI Area	2,418.22 u2	8.10 pixels			
LG Control						
	ROI 1	ROI 2	ROI 3	ROI 4	ROI 5	Average
Hoechst grey scale	25.73	21.36	20.89	24.14	30.39	24.502
OCT1 grey scale	25.74	17.25	21.72	15.84	13.11	18.732

Ratio	1.00038865	0.80758427	1.03973193	0.65617233	0.43139191	0.78705382
	ROI Area	2,418.22 u2	8.10 pixels			
LG 0.5mM						
	ROI 1	ROI 2	ROI 3	ROI 4	ROI 5	Average
Hoechst grey scale	20.73	33.2	26.83	18.43	20.19	23.876
OCT1 grey scale	24.8	20.86	23.56	20.35	23.1	22.534
Ratio	1.19633382	0.628313253	0.87812151	1.10417797	1.14413076	0.99021546
	ROI Area	2,418.22 u2	8.10 pixels			
LG 3.0mM						
	ROI 1	ROI 2	ROI 3	ROI 4	ROI 5	Average
Hoechst grey scale	12.59	20.06	11.58	12.96	18.3	15.098
OCT1 grey scale	15.88	15.95	15.74	17.83	18.24	16.728
Ratio	1.26131851	0.795114656	1.35924007	1.3757716	0.99672131	1.15763323
	ROI Area	2,418.22 u2	8.10 pixels			

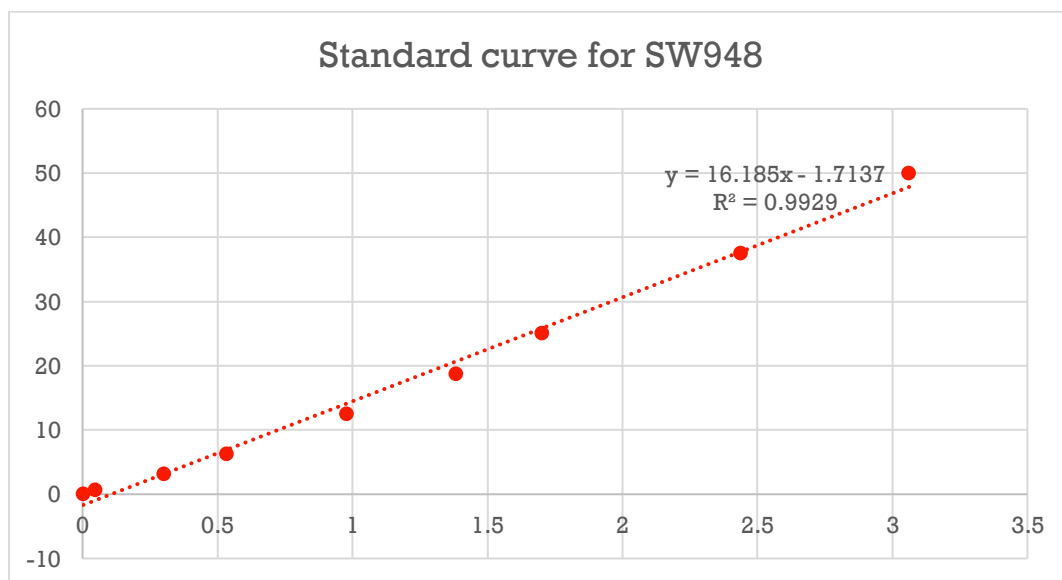
SW948 48 hours

HG Control						
	ROI 1	ROI 2	ROI 3	ROI 4	ROI 5	Average
Hoechst grey scale	7.34	21.2	9.05	14.08	3.89	11.112
OCT1 grey scale	8.68	23.82	15.35	19.25	6.96	14.812
Ratio	1.18256131	1.123584906	1.6961326	1.3671875	1.78920308	1.43173388
	ROI Area	2,418.22 u2	8.10 pixels			
HG 0.5mM						
	ROI 1	ROI 2	ROI 3	ROI 4	ROI 5	Average
Hoechst grey scale	9.35	10.81	11.34	10.54	8.51	10.11
OCT1 grey scale	18.51	19.49	15.4	22.1	18.02	18.704
Ratio	1.97967914	1.802960222	1.35802469	2.09677419	2.11750881	1.87098941
	ROI Area	2,418.22 u2	8.10 pixels			
HG 3.0mM						
	ROI 1	ROI 2	ROI 3	ROI 4	ROI 5	Average
Hoechst grey scale	14.2	8.99	12.76	15.95	15.26	13.432
OCT1 grey scale	10.51	17.35	24.82	20.98	20.37	18.806
Ratio	0.74014085	1.929922136	1.94514107	1.3153605	1.33486239	1.45308539
	ROI Area	2,418.22 u2	8.10 pixels			
LG Control						
	ROI 1	ROI 2	ROI 3	ROI 4	ROI 5	Average
Hoechst grey scale	18.88	12.44	13.75	15.72		15.1975
OCT1 grey scale	36.96	48.24	44.77	59.62		47.3975
Ratio	1.95762712	3.877813505	3.256	3.79262087		3.22101537
	ROI Area	2,418.22 u2	8.10 pixels			
LG 0.5mM						
	ROI 1	ROI 2	ROI 3	ROI 4	ROI 5	Average
Hoechst grey scale	14.9	12.46	15.62		17.29	15.0675
OCT1 grey scale	36.21	31.88	35.74		41.64	36.3675
Ratio	2.43020134	2.55858748	2.28809219		2.40832851	2.42130238
	ROI Area	2,418.22 u2	8.10 pixels			
LG 3.0mM						
	ROI 1	ROI 2	ROI 3	ROI 4	ROI 5	Average
Hoechst grey scale	17.01	18.89	18.72	20.48	15.46	18.112
OCT1 grey scale	47.67	36.68	27.85	41.6	38.84	38.528
Ratio	2.80246914	1.941768131	1.48771368	2.03125	2.51228978	2.15509814
	ROI Area	2,418.22 u2	8.10 pixels			

Seahorse standard curve used for normalisation of data on Wave



Appendix Figure 1 Standard curve for SW1116 to normalise seahorse data



Appendix Figure 2 Standard curve for SW948 to normalise seahorse data

